INVESTIGATION OF RESPONSE OF LOAD-FREQUENCY CONTROLLER IN TWO AREA RESTRUCTURED SYSTEM WITH NON-LINEAR GOVERNOR CHARACTERISTICS

A Dissertation submitted in fulfillment of the requirements for the Degree

of

MASTER OF ENGINEERING

in

POWER SYSTEMS

Submitted by

VEENA YADAV
Regd. No.: 801341028

Under the Guidance of

Ms. Manbir Kaur
Associate Professor, EIED

2015

Electrical and Instrumentation Engineering Department
Thapar University, Patiala
(Declared as Deemed-to-be-University u/s 3 of the UGC Act., 1956)
Post Bag No. 32, Patiala – 147004
Punjab (India)

DECLARATION

I hereby certify that the work which is presented in dissertation entitled, "**Investigation of Response of Load Frequency Controller in Two Area Restructured System with Non-Linear Governor Characteristics**", in partial fulfillment of the requirements for the award of the degree of Master of Engineering in Power Systems, submitted to Electrical & Instrumentation Engineering Department of Thapar University, Patiala is as authentic record of my own work carried under the supervision of **Ms. Manbir Kaur**. It refers others researcher's work which are duly listed in the reference section. The matter contained in this dissertation has not been submitted, neither in part nor in full to any other degree to any other university or institute except as reported in text and references.

Veena Yadav

Place: Patiala

(VEENA YADAV)

Date: 15-07-2015

Roll No.: 801341028

It is certified that the above statement made by the student is correct to the best of my knowledge and belief.

Manbir Kaur

(Ms. MANBIR KAUR)
Associate Professor
Electrical & Instrumentation Engineering Department
Thapar University, Patiala

Date: 15.7.15

Countersigned by:

Head
Electrical & Instrumentation Engineering Department
Thapar University, Patiala

Dean (Academic Affairs)
Thapar University, Patiala

ACKNOWLEDGEMENT

Words are often less to revels one's deep regards. With an understanding that work like this can never be the outcome of a single person. I take this opportunity to express my profound sense of gratitude and respect to all those who helped me through the duration of this work.

I am very thankful to **Dr. Prakash Gopalan**, Director of Thapar University, Patiala for providing the facilities for the completion of M.E. I express my deep sense of gratitude towards **Dr. Ravinder Aggarwal**, Head of the Department of Electrical & Instrumentation Engineering, Thapar University, Patiala who has been a constant source of inspiration for me throughout this work.

I would like express my gratitude and thanks to supervisor, **Ms. Manbir kaur**, Associate Professor, Department of Electrical and Instrumentation Engineering, Thapar University, Patiala, for her patient guidance and support through this work. It was an honor and privilege to work under her as a student. She also provides the help in technical writing and presentation style and I found her guidance to be extremely valuable.

I am also thankful to my batch mates who devoted their valuable time for the successful completion of dissertation. I extend my gratitude to the researchers and scholars whose hours of toil have produced the papers that I have utilized in my project.

Lastly, I would like to thank my parents for their years of unyielding love and encouragement. They have always wanted the best for me and admire their determination and sacrifice.

Veena Yadav

(801341028)

TABLE OF CONTENTS

TABLE OF CONTENTS (continued)

TABLE OF CONTENTS (continued)

TABLE OF CONTENTS (continued)

LIST OF TABLES

LIST OF TABLES (continued)

LIST OF TABLES (continued)

LIST OF FIGURES

LIST OF FIGURES (continued)

LIST OF ABBREVIATIONS

Apfs	Area participation factor
ACE	Area control error
AGC	Automatic Generation control
Cpf	Contract participation factor
DISCO	Distribution companies
GENCO	Generating companies
GA	Genetic Algorithm
DPM	DISCO participation matrix
ID	Integral-derivative
IDD	Integral double derivative
ISO	Independent Service operator
IPP	Independent power producer
LFC	Load Frequency control
PI	Proportional-integral
PID	Proportional integral derivative
PCS	Power conversion system
SMES	Superconducting magnetic energy storage
SSSC	Static synchronous series compensator
TCPS	Thyristor controlled phase shifter
TRANSCO	Transmission companies
VIU	Vertical integrated utility
VSC	Variable structure controller
Z-N	Ziegler-Nichols

ABSTRACT

The objective of automatic generation control (AGC) is to maintain the system frequency and tie-line flows within the scheduled values. Adaptive control of frequency has become more significant owing to increased size, complexity and restructure of power system. In this dissertation, a framework of automatic generation control with linear and non-linear governor characteristics in restructured power system has been presented. Conventional AGC with non-linear governor characteristics is reported to be dynamically unstable. To stabilize the frequency and tie-line power flow oscillations, the frequency stabilizer equipped with energy storage system is modeled. The gains of the integral controller and PID controller and parameters of frequency stabilizer are optimized using meta heuristic technique namely Genetic Algorithm. The transient response of optimized load frequency controller is simulated for two-area system comprising non-linear hydro-hydro and thermal-thermal systems. The response of simulated model is also studied under different Poolco transactions and bilateral transactions in restructured electricity market.

CHAPTER 1
INTRODUCTION

1.1 OVERVIEW

Generally, an interconnected system consists of two or more than two areas in which the generation within each area is controlled for maintaining the scheduled power interchange due to load disturbances in any area. The power and frequency control is referred to as load-frequency control (LFC).

The primary objective of AGC is to regulate the frequency of the interconnected areas to the actual frequency and the maintenance of real power exchange between control areas within the permissible limits specified by load-ability limits of tie-lines by the modified generator outputs. One of another objective is to gain the maximum economy by effective distribution of generation in various areas.

As the size and complexity of the power system is growing day by day, automatic generation control (AGC) studies are usually carried out with different kinds of controllers which are used as the supplementary control. Such intensive studies are required to reduce the chances of black outs due to spread of oscillations to wider areas. Traditionally investigations have been carried out with the help of classical controllers for example, PI, ID, PID, and IDD. In order to improve the performance of the system in terms of speed of response, steady state error, overshoot and undershoot etc., most of the modern power systems are applied with the artificial intelligence technique based controllers in which the gains of the conventional controllers are optimized with the help of meta heuristic techniques such as, fuzzy system theory, neural network and genetic algorithm etc..[8] Mostly AGC pertains to a traditional interconnected hydro-thermal system with linear governor characteristics. Lesser attention has been devoted to AGC of an interconnected hydro–hydro system involving hydro subsystems of widely different characteristics. Further the generator rotors are the only inertial systems that act as energy storage system. The study of these controllers is carried out in various kinds of interconnected areas which include thermal-thermal system, thermal-hydro system, thermal-nuclear system, thermal-diesel system, thermal-PV cells system, thermal- wind turbine system and hydro-hydro system. But in hydro-hydro system the normal AGC operation fails to make the steady-state deviations of frequency and power to zero. [13] Variety of equipment connected in modern

power system imposes serious problems to controllers to damp out the rotor oscillations. In order, to overcome this energy storage devices such as Superconducting magnetic energy storage (SMES) is provided to overcome inter-area oscillations and Thyristor controlled phase shifter (TCPS) for damping the transmission line oscillations. [5]

Competitive electricity markets in deregulated environment, the Independent service operator (ISO has to provide a large number of ancillary services for the stability and secure operation of a power system. One of this is the "frequency regulation" based on LFC. [15] In this new paradigm of vertically integrated utilities, a DISCO (distribution companies) can contract individually with a GENCO (generation companies) for power exchange is supervised by ISO. The AGC is designed in a restructured electricity market to consider various transactions such as PoolCo and bilateral (GENCO of one area can contract DISCO of other control areas) and combination of these two. The frequency deviations caused by the mismatching of actual demand and contracted demand and these deviations will cause AGC to re-allocate GENCOs according to their participation factors (*pf*). [4]

Several advancements has been reported in order to stabilize the frequency and tie-line variations of AGC, when there is a sudden demand of load, which include TCPS and SMES [9]. TCPS lies in sequence with tie-line which reduces the oscillations by modifying the phase angle. However SMES released its stored energy immediately to fulfill the sudden demand of load and charge back to its initial value current when the governor work starts. [10]

1.2 LITERATURE SURVEY

In the previous decades there are many modifications reported in the structure of AGC in various areas. The modifications presented in the field of finding the gain, bias of frequency and various different fields of power system. However, the limited investigations are presented in the area of two-area interconnected system with non-linear governor characteristics.

S.P. Ghoshal *et al.* [4] have discussed the AGC in multiple hydro-hydro units in deregulated market structure. The resultant high frequency oscillations occur due to the application of step load and the system is not able to get the stable state. Therefore, to suppress the frequency oscillations TCPS-SMES coordination has been evaluated in the restructured system.

Praghnesh Bhatt *et al.* [5] have discussed the performance of AGC in multiple-unit hydro-hydro system. When the step load is applied in order to stabilize the frequency and power

oscillations static synchronous series compensator (SSSC) or TCPS accompanied with SMES is proposed.

P.S. Kulkarni *et al.* [8] have proposed the method of tuning the gains of a variable structure controller (VSC) by genetic algorithm and the step disturbance in load is applied as input. The improvement is represented in the output response of system and the controller is vigorous to large disturbances and become insensible to large variations in parameters.

D. Das *et.al* [9] has discussed the applications of TCPS in hydro-thermal system. This control strategy is proposed for controlling the system frequency and tie-line oscillations by controlling the phase angle of TCPS. The analysis shows that the TCPS is able in damping out the oscillations during sudden application of load.

D.P Kothari *et al.* [12] have presented the critical literature review on AGC which consists of several structures. The basis of these is linear power system model compared with non-linear. Further the differences causes in the area performance on adding traditional and intelligence has also been discussed.

K.C. Divya *et al.* [13] have discussed the difficulties in AGC of hydro-hydro system. It concludes that the traditional AGC system fails to work in the hydro-hydro system. The Eigen values of the area consist of positive parts which determine the instability of the hydro-hydro system. The overcome of this difficulty is done by considering small variation in each area and considers both units as single unit.

Vaibhav Donde and M.A Pai [15] have modified the classical AGC technique so as to find out the application in deregulated environment. In deregulated market trends the power is transferred at competitive prices. So, each distributing unit has the freedom to contract with any generating unit which is done with the help of DPM matrix.

S.C Tripathy and K.P Juengst [17] have discussed the application of SMES in the AGC. The function of the SMES is applied to two-area system having reheat turbine units with the governor nonlinearities. It has been noticed that SMES is capable to deal with the rise in the power of the system.

G.Sheble *et al.* Part I [18] have discussed about the change required in the classical AGC technique for its application in the deregulated environment. It also highlighted the difference between VIU structure and deregulated environment. In this structure all possible market conditions based on the load transactions are included for the business purpose.

Kundur [22] has discussed about the response in the area of the steam units when there is sudden application of step change in load occur which further compared with responses developed from hydraulic units. The minimization of the deviations is done by applying the integrator in the feedback path.

Jaleeli *et al.* [23] have described the functioning of traditional AGC system. When there is a sudden rise in the load demand it causes the mismatching of power in the system which causes frequency deviations. To overcome this governor action takes place and lowered down the mismatch. It also provide an overview about the various generating actions types and there function during sudden application of the load. The differentiation of these units is done on the basis of AGC signal response.

Athay [26] has explained the basic function of the AGC system with ACE to minimize the oscillations occurs in the area. As it is known previously only the governor is responsible for getting back the system to stable state. For the desired generation and achieving maximum economy it is required that ACE should be zero.

Kwanty *et al.* [27] have presented an approach to track the optimal error in LFC. It also includes the power deviations due to the sudden application of the load. The drawback of the thermal energy system and sources has also been discussed.

Cohn [29] has suggested various techniques so that the transferring of the bulk power is improved. The basis of the technique is the addition of ACE to improve the system oscillations included the interchanging between the areas.

Fosha and Elgard [30] have discussed the application of ACE on the classical methods in which the finest value of the K_I is taken which is randomly adjusted. It has been noticed that the output response of the system is improved when integral of the ACE is applied in the feedback of the system.

In this literature survey various AGC strategies considering different areas has been discussed. The focus is given on the hydro-hydro system as in it normal AGC operation does not work. From the application point of view restructured market conditions and their effect on AGC is also discussed.

1.3 GAP IN STUDIES

The study of the literature reveals that most of the research work surrounds the thermal system as the linear structure of thermal system is easily can be stabilize with the help of normal AGC

operations. There is less consideration given to hydro-hydro system, because of the non-linear characteristics of the governor which is due to the transient droop compensation. The transient droop compensation is required for stable speed performance. Therfore, the normal AGC operation fails to make the steady state deviations of frequency and power to zero. The addition of compensators help in absorbing instant changes in power requirements and oscillations are damp out efficiently in multi control areas with hydro units having non-linear governor characteristics and units of different capacities.

1.4 DISSERTATION WORK OBJECTIVE

Following are the objectives of the work studied:

(i) To develop mathematical model of two-area interconnected system with linear governor characteristics and simulate it.

(ii) To transform the model to incorporate non-linear governor characteristics.

(iii) To develop the conventional controller design to stabilize the steady-state frequency and power deviations with the help of compensators in AGC with non-linear governor characteristics.

(iv) To implement the DPM matrix in two-area system with linear and non-linear governor characteristics under deregulated structure.

(v) To find the optimal value of controller gains and compensators parameters with the help of genetic algorithm.

1.5 ORGANIZATION OF THE THESIS WORK

The presentation of dissertation work is in following 7 chapters:

Chapter 1: deliberates the overview of the problem, brief literature survey and objectives of the study.

Chapter 2: explores the mathematical modeling of the various power system components.

Chapter 3: explains about the various controller techniques and stability of the system.

Chapter 4: discusses about the Automatic Generation control and its characteristics in Single and Two-area system with linear and non-linear governor characteristics.

Chapter 5: illustrates the formulation of AGC in deregulated environment and there effects during various transaction conditions.

Chapter 6: explains about the soft optimization technique namely genetic algorithm.

Chapter 7: concludes the simulation results of AGC in the deregulated environment.

CHAPTER 2
Automatic Generation Control

2.1 Introduction

The analysis of power system reveals that frequency sensitive units are loads and losses. The declination of frequency is occur because of the tripping of generating units or due to the addition of load blocks which causes the power variation. Initially, these variations are overcome by stored kinetic energy. As, the frequency decline loads also take less power. The equilibrium state of the larger systems is obtained when the frequency sensitive load reduces or the mismatch of trip unit output power or the added load block reduces. [21]

When the frequency changes under primary regulation, governors respond immediately. But the frequency does not get restored and settled down to a different value because of the droop of the governors. The function of Secondary regulation is performed by AGC to maintain the system frequency. The generators are provided with generation set points participating in the frequency regulation. Thus, the AGC function is the replacement of the manual control of the adjustment of generation by governors. There is also reduction in the response time of AGC because it instantly responds to load changes.

In the recent practice, LFC function of AGC is based on the tie-line bias control. In this, each area concentrates on maintaining the ACE to zero, where;

$$ACE = (T_a - T_s) - 10\beta(f_a - f_s) \quad \ldots (2.1)$$

The term ($T_a - T_s$) is the difference between the actual and the scheduled tie-line power and $10\beta(f_a - f_s)$ represents the natural response of area when frequency variations occur. The representation of the bias factor isβ. The error signal is consist of tie-line power deviations which are being summed to frequency deviations multiplied by a bias factor. The lowering and rising in the control area generation is indicated by ACE. [14]

2.2 Objectives of Automatic Generation Control

The four basic objectives of power system operation connected with AGC are: [22]

(i) To match the total generation by the system with total load of the system.

(ii) To regulate the system frequency deviations error to zero in steady-state.

(iii) To distribute system generation among the areas of interconnected system so that the net tie-line power match the scheduled tie-line power.

(iv) To distribute area generation among various units of power system so that maximum economy can be obtained.

2.3 Mathematical Modeling of Generation Area Components

The electrical energy is basically obtained with the help stored kinetic energy in water and the energy obtained from the fossil fuels. With the help of governor these sources of energy is converted in to electrical energy from the mechanical energy. The governors also help in controlling the frequency and power of the system. The relationship of the basic units such as load, generator, turbine and governor associated with power generation and control is shown in figure 2.1:

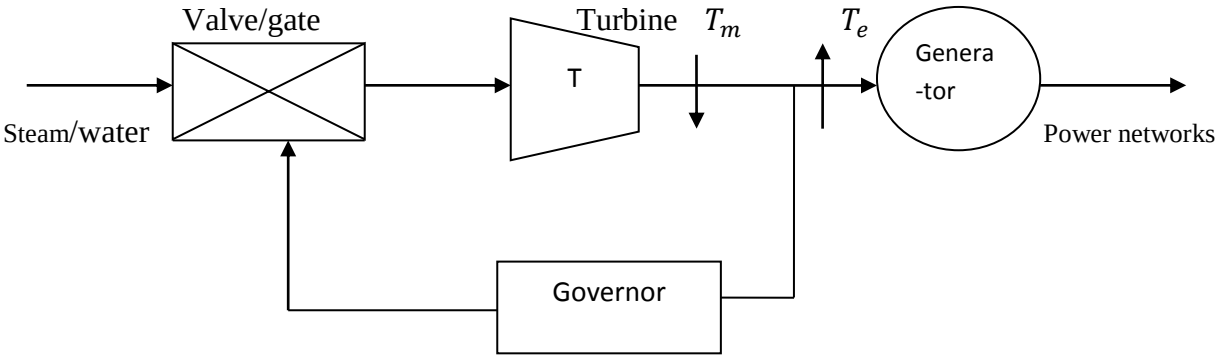

Fig2.1: Basic schematic

Fundamental approach to develop mathematical modeling of the various components connected in an area is described below:

2.3.1 Generator

When there is a change in load, there has been an instant generator's electrical torque T_e occurs. The following change will cause mismatching of T_m and T_e that is mechanical and electrical torque which causes speed variations as evaluated by using the equation of motion (2.2), the mathematical model of the generator can be modeled as [22]:

$$2H\frac{d^2}{dt^2}\Delta\delta = \Delta P_m - \Delta P_e \quad \ldots (2.2)$$

$$\frac{d}{dt}\Delta\omega_r = \Delta\delta \quad \ldots (2.3)$$

$$\frac{d}{dt}\Delta\omega_r = \frac{1}{2H}(\Delta P_m - \Delta P_e) \quad \ldots (2.4)$$

Where the power P is related to T is shown below:

$$P = \omega_r T \quad \ldots (2.5)$$

The small deviations are denoted by prefix Δ and initial condition by subscript 0 as given below:

$$P = P_0 + \Delta P \quad \ldots (2.6)$$

$$T = T_0 + \Delta T \quad \ldots (2.7)$$

$$\omega_r = \omega_0 + \Delta\omega_r \quad \ldots (2.8)$$

From equation 4,

$$P_0 + \Delta P = (\omega_0 + \Delta\omega_r)(T_0 + \Delta T) \quad \ldots (2.9)$$

The higher-order terms are neglected and the respective formed equation is given as:

$$\Delta P = \omega_0 \Delta T + T_0 \Delta\omega_r \quad \ldots (2.10)$$

So,

$$\Delta P_m - \Delta P_e = \omega_0(\Delta T_m - \Delta T_e) + (T_{m0} - T_{e0})\Delta\omega_r \quad \ldots (2.11)$$

The mechanical and electrical torque is equal in the steady state, $T_{m0} = T_{e0}$. With speed expressed in p.u., $\omega_0 = 1$. Hence,

$$\Delta P_m - \Delta P_e = \Delta T_m - \Delta T_e \quad \ldots (2.12)$$

Hence, equation (2.2) can be represented in the of block diagram form in figure 2.2:

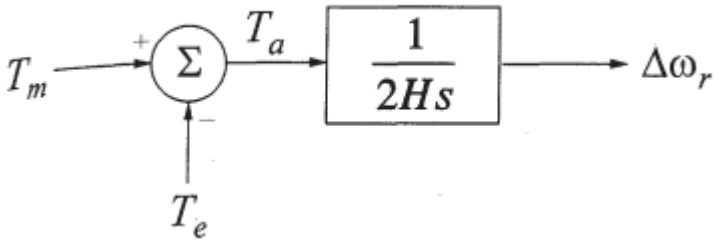

Fig2.2: Block diagram of generator

Where,

T_a = Accelerating torque (in p.u)

H= Inertia constant (in MW-sec/ MVA)

$\Delta\omega_r$ = change in speed of the rotor

2.3.2 Load

The electrical power system devices consist of variety of loads. When the resistive loads are applied the electrical power does not depend on frequency and on the application of motor loads, change in frequency occur with the change in speed of motor. The mathematical modeling of frequency-dependent load is evaluated as follow [22]:

$$\Delta P_e = \Delta P_L + D\Delta\omega_r \quad \ldots (2.13)$$

Therefore, ΔP_L is the change in non-frequency sensitive load. The damping constant D can be shown as a change in load percent when 1% frequency change occur. The block diagram of frequency-dependent load is shown in figure2.3:

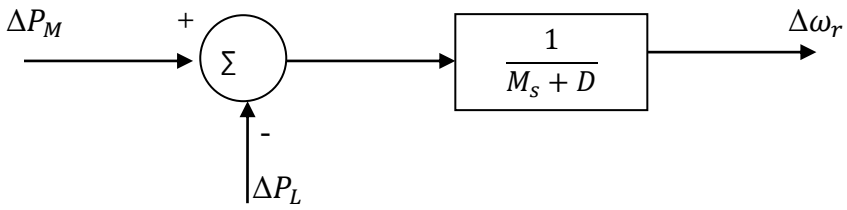

Fig2.3: Block diagram of Load

2.3.3 Turbine

2.3.3.1 Modeling of Steam Turbines

The transfer function of a steam vessel and the expression for power developed by a turbine is expressed as below:

The steam vessel continuity expression is expressed as:

$$\frac{d}{dt}W = V\frac{d}{dt}\rho = Q_{in} - Q_{out} \quad \ldots (2.14)$$

Where,

W =steam weight present in the vessel (kg)

V =volume of vessel (m^2)

ρ =steam density (kg/m^3)

Q = flow rate of steam (kg/s)

t =time (s)

Further, as the steam flow is proportional to the pressure present in the vessel, therefore

$$Q_{out} = \frac{Q_0}{P_0}P \quad \ldots (2.15)$$

Where,

P =steam pressure present in the vessel (kPa)

P_0 =rated pressure

Q_0 =rated vessel flow

As the temperature is considered as constant in the vessel,

$$\frac{d}{dt}\rho = \frac{d}{dt}P\frac{\partial}{\partial P}\rho \quad \ldots (2.16)$$

At the given temperature, the steam density change respective with pressure is represented by $/\partial P$. Therefore,

$$Q_{in} - Q_{out} = V \frac{\partial \rho}{\partial P} \frac{dP}{dt} \quad \ldots (2.17)$$

$$= V \frac{\partial}{\partial P} \rho \frac{P_0}{Q_0} \frac{dQ_{out}}{dt}$$

$$= T_{CH} \frac{dQ_{out}}{dt}$$

Where,

$$T_{CH} = \frac{P_0}{Q_0} V \frac{\partial}{\partial P} \rho$$

In Laplace form, equation may be written as,

$$Q_{in} - Q_{out} = T_{CH}\, s\, Q_{out}$$

$$\frac{Q_{out}}{Q_{in}} = \frac{1}{1+T_{CH}s} \quad \ldots (2.18)$$

Where,

T_{CH} =time constant

According to the equation (2.18), the block diagram for steam turbines can be represented as in Figure 2.4:

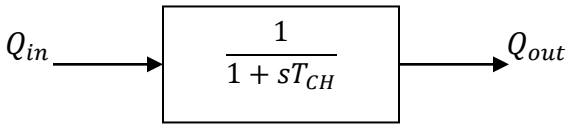

Fig2.4: Block diagram of steam turbine

2.3.3.2 Modeling of Hydraulic Turbines

The characteristics of turbines and penstock are based on the parameters given below: [28]

(a) Velocity of water in the penstock

(b) Turbine mechanical power

(c) Acceleration of water column

The water velocity in the penstock is represented as:

$$U = K_u G \sqrt{H} \quad \ldots (2.19)$$

Where,

G= gate position

U= water velocity

H= hydraulic head at gate

K_u= a constant of proportionality

If small variations are included,

$$\Delta U = \frac{\partial}{\partial H} U \Delta H + \frac{\partial}{\partial G} U \Delta G \quad \ldots (2.20)$$

Including the appropriate expressions for the partial derivatives and divide it through by

$U_0 = K_u G_0 \sqrt{H_0}$, Yields

$$\frac{\Delta U}{U_0} = \frac{\Delta H}{2H_0} + \frac{\Delta G}{G_0} \quad \ldots (2.21)$$

The mechanical power of the turbine is proportional to flow and pressure; hence,

$$P_m = K_p HU \quad \ldots (2.22)$$

Linearizing by considering small displacements, and normalize it by dividing with $P_{m0} = K_p H_0 U_0$ we have,

$$\frac{\Delta P_m}{P_{m0}} = \frac{\Delta H}{H_0} + \frac{\Delta U}{U_0} \quad \ldots (2.23)$$

Substituting for ΔU gives,

$$\Delta P_m = 1.5\Delta H + \Delta G \quad \ldots (2.24)$$

If we substitute for ΔH it may be written as,

$$\Delta P_m = 3\Delta U - 2\Delta G \quad \ldots (2.25)$$

The accelerating water column is characterized by Newton's second law, is represented as

$$\rho LA \frac{d\Delta U}{dt} = -A(\rho a_g)\Delta H \quad \ldots (2.26)$$

Where,

L= length of pipe

A= pipe area

ρ = mass density

a_g= acceleration due to gravity

ρ LA= water mass in the pipe

ρ a_gΔH= change in the pressure of the turbine gate

t= time in seconds

Dividing both sides by aρ $a_g H_0 U_0$, the accelerating equation in normalized form becomes,

$$\frac{LU_0}{a_g H_0} \frac{d}{dt}\left(\frac{\Delta U}{U_0}\right) = -\frac{\Delta H}{H_0} \quad \ldots (2.27)$$

$$T_w \frac{d\Delta U}{dt} = -\Delta H \quad \ldots (2.28)$$

And $T_w = \frac{LU_0}{a_g H_0}$

Where,

T_w =water starting time

The correlation of velocity change and gate position as,

$$T_w \frac{d\Delta\bar{U}}{dt} = 2(\Delta\bar{G} - \Delta\bar{U}) \quad \ldots (2.29)$$

Replacing d/dt by s,

$$T_w s\Delta\bar{U} = 2(\Delta\bar{G} - \Delta\bar{U}) \quad \ldots (2.30)$$

$$\Delta\bar{U} = \frac{1}{1+s\frac{T_w}{2}}$$

Substituting the $\Delta\bar{U}$, we get

$$\frac{\Delta\overline{P_m}}{\Delta\bar{G}} = \frac{1-T_w s}{1+0.5sT_w} \quad \ldots (2.31)$$

According to equation (2.31), the block diagram for hydraulic turbines can be represented as shown in figure 2.5:

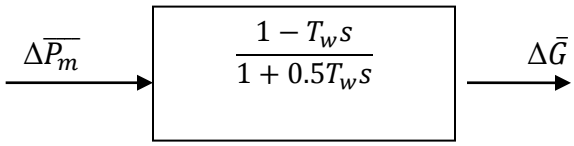

Fig2.5: Block diagram of hydraulic turbine

2.3.4 Governor

The analysis of small signal is introduced around the steady-state condition for developing the simulation model. The schematic and parameters of the governor system is shown in figure 2.6 [21]:

The governing system consists of following components:

Speed Governor: It is represented by the fly-balls which move vertically up or down with the change of speed as it is proportional with changing speed.

Linkage Mechanism: The linkage mechanism is done with the help of L_1, L_2, L_3, L_4 linkage arms. The points on these arms are represented with A, B, C, D, and E. The function of this mechanism is to provide progress in the valves of the turbine with the help of hydraulic amplifier which is proportional to the changing speed of shaft.

Speed Changer: There is a vertical rotating screw for the movement up and down of A. The servo-motor drive this screw. The point A is adjusted so that nominal frequency can be obtained.

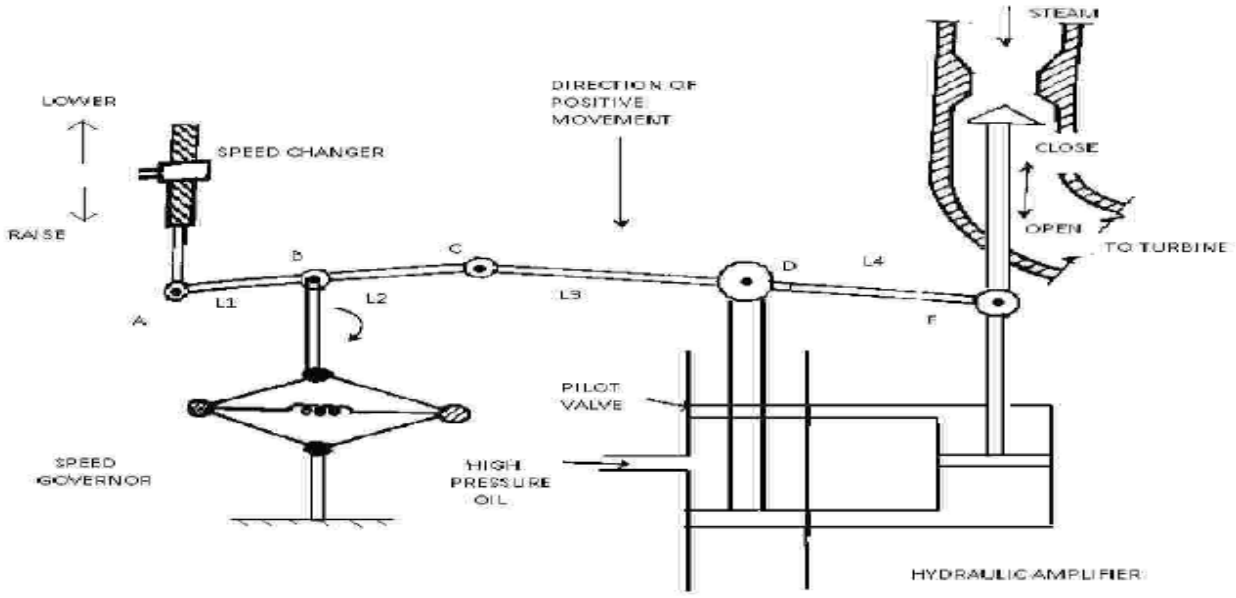

Fig2.6: Schematic Representation of Speed Governing System

The change in settings of power ΔP_{ref} is due to the position change ΔY_A of A. Similarly, the change in settings of valve position ΔP_v causes changes in ΔY_c due to which turbine power changes ΔP_t.

The following procedure occurs during the working of the system:

1 If the speed changer makes a small movement in the downward direction so that of point A.

2 when there is no change in speed kept point B as fixed. However, due to the movement of point A points C move by ΔY_c and point D move by ΔY_d respectively. Because of this oil starts flowing through the pilot valve which move it downward direction and the movement of steam valve by ΔY_c.

For small deviations, the following expression can be build:

$$\Delta Y_c = K_1 \Delta f - K_2 \Delta f \quad \ldots (2.32)$$

$$\Delta Y_D = K_3 \Delta f - K_4 \Delta P_{ref} \quad \ldots (2.33)$$

The progress of ΔY_E is obtained by taking division of volume of the oil and the cross-section area of the piston as follows:

$$\Delta Y_E = K_5 \int Y_D \, dt \quad \ldots (2.34)$$

Eliminate ΔY_c and ΔY_D and take the Laplace transform

$$\Delta Y_E(s) = \frac{K_2 K_3 \Delta P_{ref}(s) - K_1 K_3 \Delta f(s)}{K_4 + \frac{s}{K_5}} \quad \ldots (2.35)$$

The equations may be expressed in the following way:

$$\Delta P_{ref}(s) - \frac{1}{R} f(s) = \Delta Y_E(s) \quad \ldots (2.36)$$

$$\frac{K_{SG}}{1+sT_{SG}} \left[\Delta P_{ref}(s) - \frac{1}{R}\Delta f(s)\right] = \Delta Y_E(s) \quad \ldots (2.37)$$

$$G_{SG} \left[\Delta P_{ref}(s) - \frac{1}{R}\Delta f(s)\right] = \Delta Y_E(s)$$

Where,

$R = \frac{K_2}{K_1}$ Speed regulation

$K_{SG} = \frac{K_2 K_3}{K_4}$ Gain of the governor unit

$T_{SG} = \frac{1}{K_4 K_5}$ Time constant of the governor unit

$G_{SG}(s)$ is the transfer function

2.3.4.1 Governor Droop Characteristics

The power deficit of the load side is taken from the turbine's rotating energy. The turbine's kinetic energy because of this reason i.e. the machine stored energy is reduced and a signal is sent from governor to supply more volumes of water or steam to compensate speed deficiency and to increase the speed of prime mover [21]. The graph of the droop characteristics shown in figure 2.7:

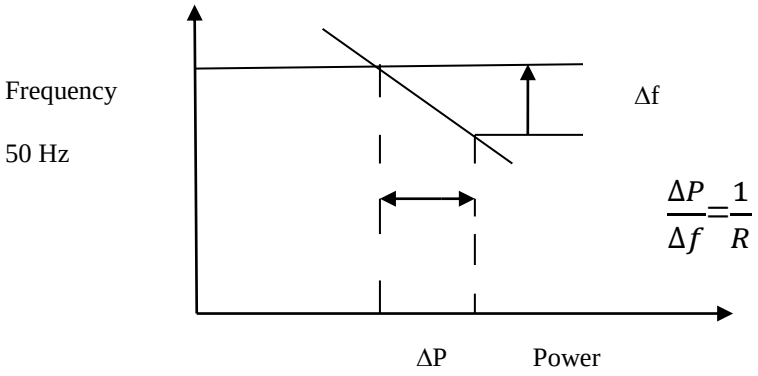

Fig2.7: Graphical representation of speed regulation by governor

The curve slope is represented by R which is speed regulation. Governors typically have the regulation of speed 5-6% from no-load to full load.

The block diagram for the speed governing mechanism with reference to equation (2.37) is represented as in figure 2.8:

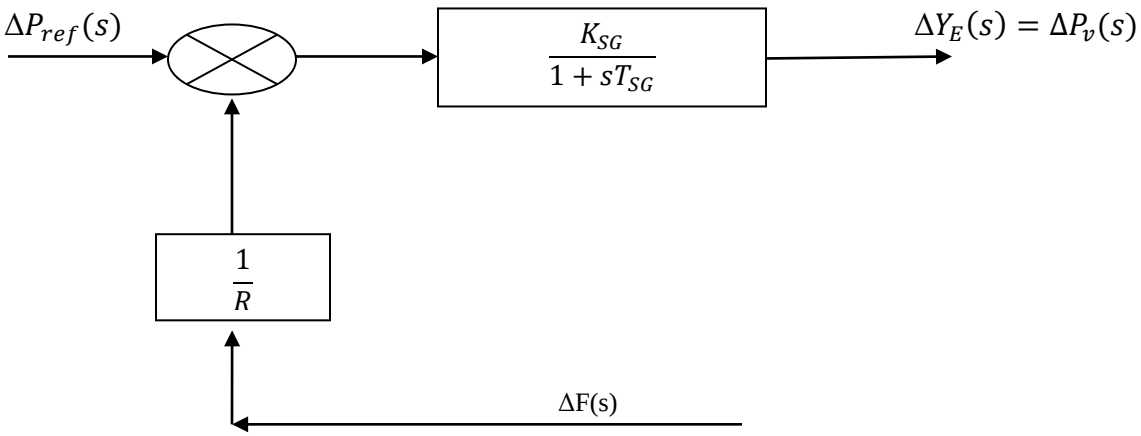

Fig2.8: Block diagram of the speed governing mechanism

2.3.4.2 Hydraulic Governor

The response of a steam turbine has no such peculiarity as exhibited by a hydraulic turbine because of water inertia. The governing requirements of steam turbines, in this respect are more straightforward. Therefore, the control action is stable with normal speed regulation and there is no purpose for transient droop. In hydraulic units for stable speed control performance governors require transient droop compensation. At the foot of the penstock because of change in the position of gate it produces an initial short-term power change in turbine that is opposite to sought, the governors of hydraulic-turbine are designed to have relatively long resetting times with large transient droop. Under isolated operating conditions it ensures stable frequency regulation. Consequently, the response of a hydraulic-governor unit to changes in speed-changer setting or to speed change is relatively low. [5]

The governing function is realized by using the components of mechanical and hydraulic system. Various parameters such as permanent droop, speed sensing is obtained with the help of hydraulic components. A simplified schematic of a mechanical-hydraulic governor is shown in figure 2.9:

The relation of the relay valve and gate servomotor is provided as:

$$\frac{g}{a} = \frac{K_1}{s} \quad \ldots (2.38)$$

And, the valve and servo transfer function is represented as:

$$\frac{a}{b} = \frac{K_2}{1+sT_p} \quad \ldots (2.39)$$

Where, K_2 is the lever ratio

T_p is determined with the help of port in the areas of the pilot valve

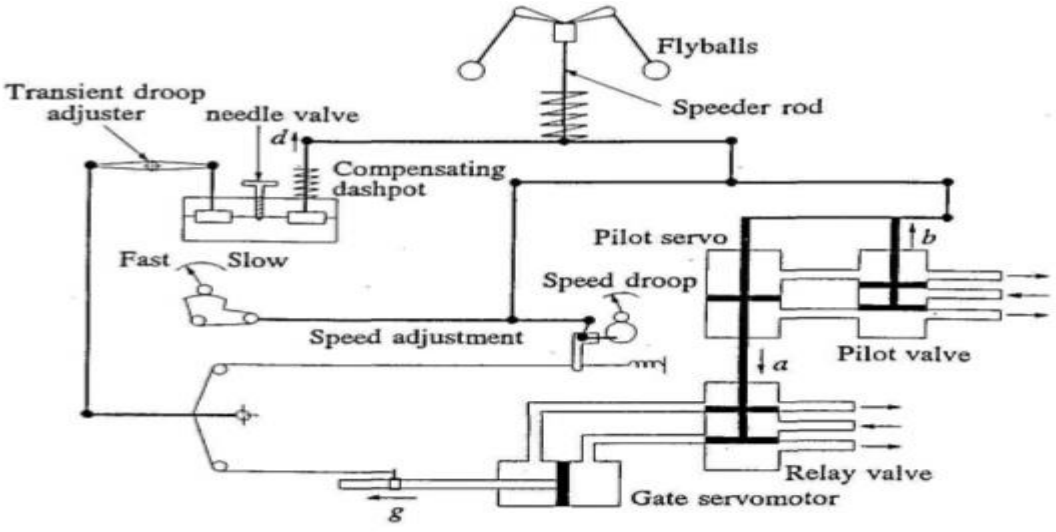

Fig2.9: Schematic of a mechanical-hydraulic governor for a hydro turbine

Combining equations yields

$$\frac{g}{a} = \frac{K_1 K_2}{s(1+sT_p)} = \frac{K_s}{s(1+sT_p)} \quad \ldots (2.40)$$

Where,

K_s= Servo gain

T_p= Pilot valve/servomotor time constant

For providing transient droop compensation a dash pot is used. The transfer function of dashpot is,

$$\frac{d}{g} = R_T \frac{sT_R}{1+sT_R} \quad \ldots (2.41)$$

The representation of the governor system with equation (2.42) is shown in figure 2.10:

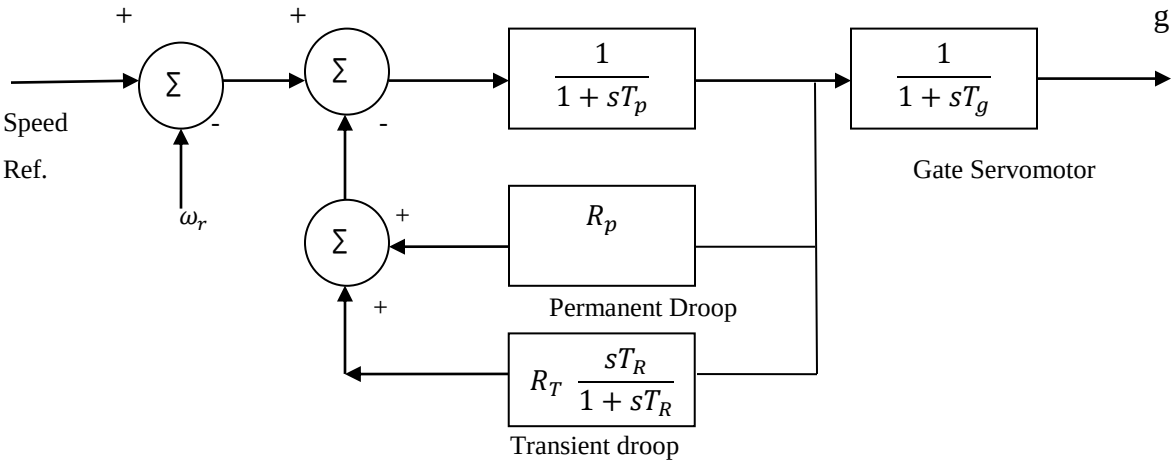

Fig2.10: Block diagram of Hydraulic Governor

The transfer function is given as:

$$\frac{\Delta G}{\Delta \omega_r} = \frac{1}{1+sT_G}\frac{1+sT_R}{1+s(\frac{R_T}{R_p})T_R} \quad \ldots (2.42)$$

2.3.5 Compensators

The interconnected system having non-linear governor characteristics when application of load disturbances occur causes disturbance in the frequency. In order for the compensation of load variations and stabilization of the area frequency oscillations frequency controllers such as TCPS in coordination with SMES is provided, where TCPS will help in damping out the tie-line power oscillations and SMES will help in damping the area oscillations. The detailed discussion about these frequency controllers is given below [5]:

2.3.5.1 Linearized Model of TCPS

The representation of hydro-hydro system with application of TCPS is shown in the figure 2.11:

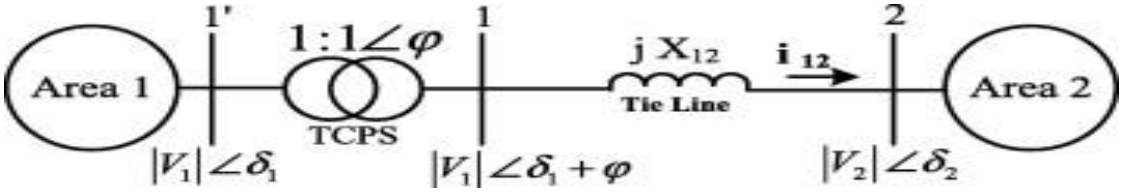

Fig2.11: Schematic of TCPS in series with the tie-line

Neglecting TCPS, the change in tie-line power can be represented as:

$$\Delta P^0_{tie12}(s) = \frac{T_{12}}{s}[\Delta\omega_1(s) - \Delta\omega_2(s)] \quad \ldots (2.43)$$

The expression of current with the application of TCPS can be represented as:

$$I_{12} = \frac{|V_1|<(\delta_1+\varphi) - |V_2|<(\delta_2)}{jX_{12}} \quad \ldots (2.44)$$

$$P_{tie12} - jQ_{tie12} = V_1^* I_{12} \quad \ldots (2.45)$$

Therefore,

$$P_{tie12} - jQ_{tie12} = \frac{|V_1||V_2|}{X_{12}}\sin(\delta_1 - \delta_2 + \varphi) - j\frac{[|V_1|^2 - |V_1||V_2|\cos(\delta_1 - \delta_2 + \varphi)]}{X_{12}} \quad \ldots (2.46)$$

Separating the real parts we get,

$$P_{tie12} = \frac{|V_1||V_2|}{X_{12}}\sin(\delta_1 - \delta_2 + \varphi) \quad \ldots (2.47)$$

$$\Delta P_{tie12} = \frac{|V_1||V_2|}{X_{12}}\cos(\delta_1^0 - \delta_2^0 + \varphi^0)\sin(\Delta\delta_1 - \Delta\delta_2 + \Delta\varphi) \quad \ldots (2.48)$$

$(\Delta\delta_1 - \Delta\delta_2 + \Delta\varphi) \approx 0.$

Hence, $\sin(\Delta\delta_1 - \Delta\delta_2 + \Delta\varphi) \approx (\Delta\delta_1 - \Delta\delta_2 + \Delta\varphi)$

Therefore,

$$\Delta P_{tie12} = \frac{|V_1||V_2|}{X_{12}}\cos(\delta_1^0 - \delta_2^0 + \varphi^0)(\Delta\delta_1 - \Delta\delta_2 + \Delta\varphi) \quad \ldots (2.49)$$

$$T_{12} = \frac{|V_1||V_2|}{X_{12}}\cos(\delta_1^0 - \delta_2^0 + \varphi^0) \quad \ldots (2.50)$$

Thus, the equation reduces to;

$$\Delta P_{tie12} = T_{12}(\Delta\delta_1 - \Delta\delta_2 + \Delta\varphi) \quad \ldots (2.51)$$

Therefore,

$$\Delta P_{tie12} = T_{12}(\Delta\delta_1 - \Delta\delta_2) + T_{12}\Delta\varphi \quad \ldots (2.52)$$

As,

$$\Delta\delta_1 = \int \Delta\omega_1 dt \text{ And } \Delta\delta_2 = \int \Delta\omega_2\, dt \quad \ldots (2.53)$$

Therfore, we get

$$\Delta P_{tie12} = T_{12}(\int \Delta\omega_1 dt - \int \Delta\omega_2 dt) + T_{12}\Delta\varphi \quad \ldots (2.54)$$

On taking the Laplace of above equation we get,

$$\Delta P_{tie12}(s) = \frac{T_{12}}{s}[\Delta\omega_1(s) - \Delta\omega_2(s)] + T_{12}\Delta\varphi(s) \quad \ldots (2.55)$$

The phase shifter angle $\Delta\varphi(s)$ is shown as:

$$\Delta\varphi(s) = \frac{K_\varphi}{1+sT_{ps}}\Delta Error(s) \quad \ldots (2.56)$$

Therefore,

$$\Delta P_{tie12}(s) = \frac{T_{12}}{s}[\Delta\omega_1(s) - \Delta\omega_2(s)] + T_{12}\frac{K_\varphi}{1+sT_{ps}}\Delta Error(s) \quad \ldots (2.57)$$

Thus,

$$\Delta\varphi(s) = \frac{K_\varphi}{1+sT_{ps}}\Delta\omega_1(s) \quad \ldots (2.58)$$

And the tie line power deviations represented as,

$$\Delta P_{tie12}(s) = \frac{T_{12}}{s}[\Delta\omega_1(s) - \Delta\omega_2(s)] + T_{12}\frac{K_\varphi}{1+sT_{ps}} \quad \ldots (2.59)$$

$$\Delta P_{tie12}(s) = \Delta P_{tie12}^0(s) + \Delta P_{TCPS}(s)$$

Where,

$$\Delta P_{TCPS}(s) = T_{12}\frac{K_\varphi}{1+sT_{ps}} \quad \ldots (2.60)$$

The input for the TCPS as a controller is provided by the rotor speed variations of the area of interconnected system where, K_f is the nominal system frequency gain block. The two parameters are stabilization gain K_φ and T_{ps}. These parameters are to be optimized in order to get

the optimized design of the TCPS. The TCPS structure in the form of frequency controller is shown in figure 2.12:

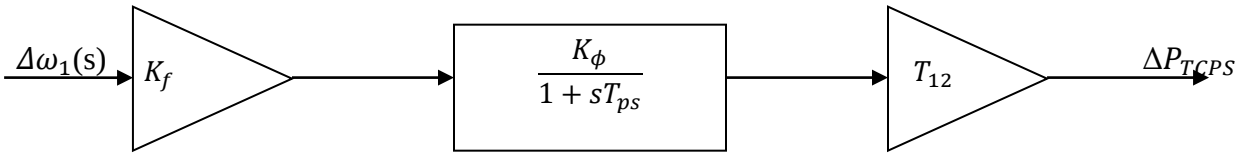

Fig2.12: Structure of TCPS as a frequency controller

2.3.5.2 Linearized SMES

In normal operating conditions the Power conversion system will charge the SMES coil to its full value. The PCS consists of inverter/rectifier unit which help in the charging and discharging of the coil from the main grid. The electromagnetic field is produced in the coil due to which flow of current occur. The coil is maintained at low temperature by keeping it in liquid helium. [5]

During the sudden rise of the load demand, SMES supplies its stored energy through PCS. When the other mechanism such as governor starts work then SMES is get charged to its initial value. The same kind of action occur when there is loss of load in this case SMES absorb excess energy from the system and when this excess energy is released during the steady-state conditions coil retain its normal value.

The SMES unit consists of a dc inductor, a 12-pulse bridge type ac/dc converter. It also consists of a Y-Y/Δ step down transformer. The control of charging and discharging is done with the help of commutation angle (γ). The representation of SMES is shown in figure 2.13. [9]

- If γ<90^0 it works in the converter mode that is charging mode
- If γ >90^0 it works in the inverter mode that is discharging mode

When the variation of load occurs SMES comes in to action to minimize the frequency variations. The I_d current of the bridge cannot reverse it direction. However, the output ΔP_{SM} depends on the firing angle. The energy stored in superconducting inductor is,

$$E_{SM} = E_{SMO} + \int_{t_0}^{t} P_{SM}(\tau)d\tau \quad \ldots (2.61)$$

Where, $E_{SM} = \frac{1}{2}L_{do}^2$ is the inductor's initial energy. By applying a low positive voltage the inductor get charged by rated current I_{do}. When the current attains its rated value, voltage reduces to zero; it is maintained constant because of the superconducting nature of the coil. The schematic arrangement of SMES is shown in figure 2.13.

The DC voltage across the inductor is represented as:

$$E_d = 2U_{d0}\cos\gamma - 2I_dR_c \quad \ldots (2.62)$$

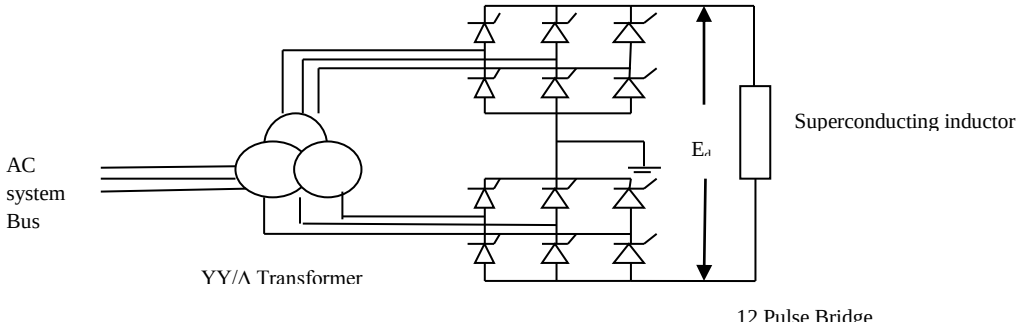

Fig2.13: SMES arrangement

The frequency deviations Δf is sensed and control the voltage E_d of SMES. The E_d becomes negative when sudden application of load occurs. Due to which frequency falls and power is send back to the area. The change in the inductor voltage is represented as:

$$\Delta E_d = [\frac{K_{SMES}}{1+sT_{SMES}}]\Delta f_i \quad \ldots (2.63)$$

The second order lead-lag compensator of SMES is shown in figure 2.14. These parameters are time constants T_{SMES}, T_1, T_2, T_3, T_4 and stabilization gain K_{SMES} for the design of the SMES are to be optimized. The placement of SMES is done at the load point.

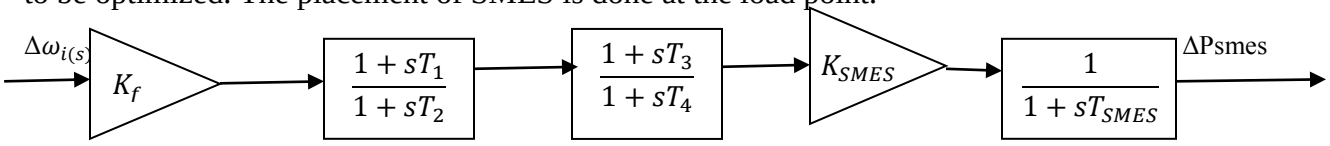

Fig2.14: Structure of SMES as a frequency controller

Hence the various components and their mathematical modeling have been developed for the further requirements of the development of the system problem.

CHAPTER 3

Controller techniques

3.1 Introduction

The performance of the system analysis depends on the test input applied to the system, or the output occurs when the response has been settled down to a steady state. The output of the system can be viewed on the basis of its parameters in time province. Basically, the output of the system is divided into two parts, (i) the initial reaction known as transient response (ii) the steady reaction known as steady state response. The characteristics of time response and its various parameters are described in figure 3.1. [6]

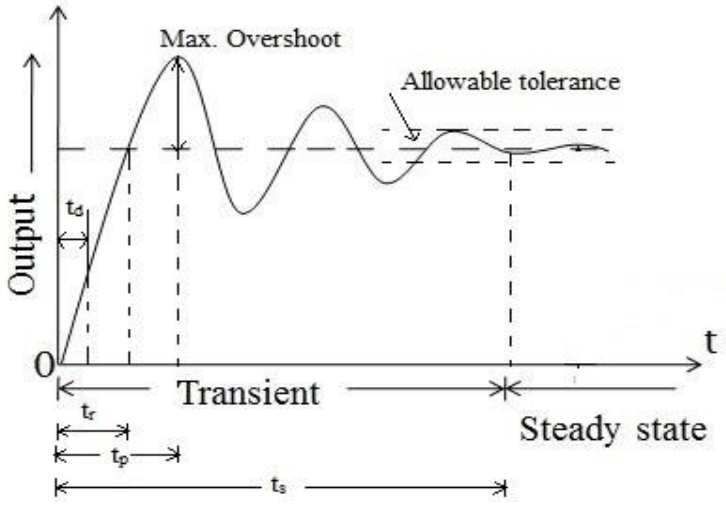

Fig 3.1: Time response of control system

The transient part of the time response curve reveals the nature of response and also gives an indication about its speed. However, the steady-state part of time response reveals about the accuracy of a control system.

3.2 Transient Response Specifications

Analysis of the transient response of the control system considered some specifications as shown in figure 3.1 which are described below:

1. **Delay time:** The time taken by the response to reach 50% of the final value for the first time, this time is known as delay time. Delay time is represented as t_d as shown in figure 3.1.

2. **Rise time:** This is represented by t_r. The rise time can be defined in two cases: (i) for underdamped system rise time is defined as the time required by the response to reach from 0 values to 100% value of final value where the value of $\varepsilon_{,}$ is less than one. (ii) For overdamped

system rise time is defined as the time required by the response to reach from 10% value to 90% value of final value where the value of ε_ι is greater than one.

3. **Peak time:** The peak is the time required by the response to reach the peak value for the first time. Peak time is represented by t_p in the given time response curve.

4. **Settling time:** Settling time is the time required by the response to reach within the specified range of about (2% to 5%) of its final value for the first time. Settling time is represented as t_s in the time response curve.

5. **Maximum overshoot:** It is defined as the maximum positive deviations of the response from its desired value where, the desired value is the steady-state value.

6. **Steady state error:** It is defined as the difference between the desired output and the actual output as the time tends to infinity.

3.3 Stability Analysis of Control system

The control system when an input is applied if the output response comes oscillating and by damping out such oscillation system get the steady-state, then the system is referred to as stable system and if the magnitude of output response is increasing and does not stabilize to the steady-state, then the system is referred to as unstable system. [7]

The absolute stability can be determined with the help of position of roots of the characteristics equation in s-plane. In second order system the nature of time response for a step input and the corresponding characteristic equation roots location are shown below:

(a) If the roots of a characteristic equation have negative real part and the output response is finite then the system is stable.

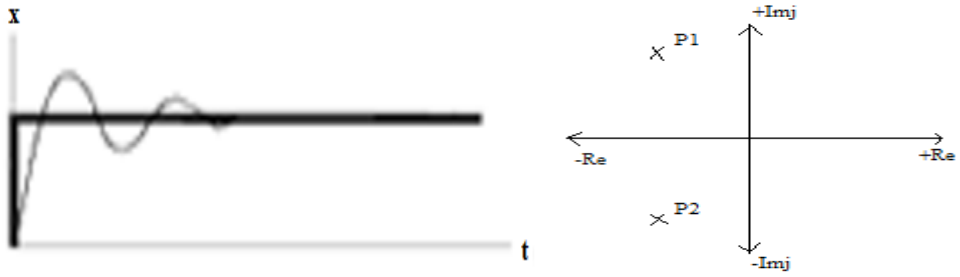

Fig 3.2: Stable

(b) The roots of the characteristic equation with positive real part lead to an infinite output response and indicate unstable system.

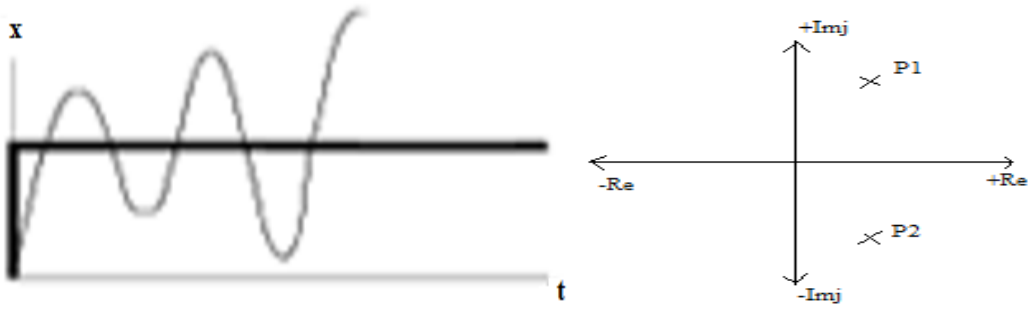

Fig 3.3 Unstable

Thus the absolute stability can be determined by examining the sign of real parts of the roots of a system characteristic equation. The system is stable when roots have negative real part and unstability occur if even one of the roots is having a positive real part.

3.3.1 State-space stability

The state space representation of multiple inputs and multiple outputs (MIMO) system is given by the equations below: [7]

$$\dot{x} = Ax + Bu \quad \ldots (3.1)$$

$$y = Cx + Du \quad \ldots (3.2)$$

The block diagram of the system based on equation (3.1) and (3.2) is shown in figure 3.4 below:

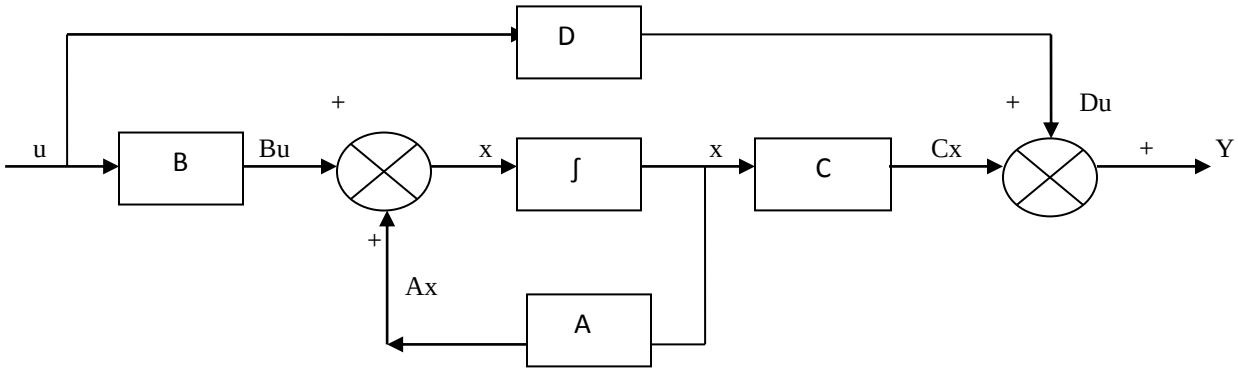

Fig 3.4: Block diagram for state equations (3.1) and (3.2)

Where, x represents the state vector, y represents the output vector, u represents control vector, A represents system matrix, B represents input matrix, C represents output matrix and D represents input-output matrix

(i) Eigen values of the system

If all the Eigen values of A (system matrix) have negative real parts then the system is called to be stable which can be calculated by considering given expression:

$$x' = Ax(t) + Bu(t) \quad \ldots (3.3)$$

If the Laplace transform is taken on both sides and consider the initial condition $x_0 = 0$;

$$sX(s) = AX(s) + BU(s) \quad \ldots (3.4)$$

By subtracting AX(s) from both side we have;

$$(sI - A)X(s) = BU(s) \quad \ldots (3.5)$$

Multiply by the inverse (sI-A)

$$X(s) = (sI - A)^{-1}BU(s) \quad \ldots (3.6)$$

Using the formula for inverse equation 3.6 can be replaced as;

$$X(s) = \frac{adj(sI-A)BU(s)}{|sI-A|} \quad \ldots (3.7)$$

Following is the condition for the system to be stabilized:

$$D(s) = |(sI - A)| = 0 \quad \ldots (3.8)$$

The substitution of ʌ in place of s will form the characteristic equation for matrix A. This gives the values for s for which equation become stable. In S-plane the requirement is that all poles will lie in the left-half for stability, therefore all the Eigen values of A should have negative real values.

3.3.2 Methods for determining stability

In a control system with feedback the stability analysis is based on finding the roots of characteristic equation in S-plane. The methods for assessing the stability of control system are:

1. **Routh-Hurwitz criterion:** This method is used for the determination of stability in higher order systems. The Hurwitz determinant of a polynomial is given below:

$$a_0 s^n + a_1 s^{n-1} + a_2 s^{n-2} + \cdots + a_n = 0 \quad \ldots (3.9)$$

For the roots of the n^{th} order polynomial given in equation 3.9 to have only negative real parts i.e. all the roots to lie in left half of s-plane it is required that the polynomials Hurwitz determinant D_k,(k=1,2,3,…..,n) be greater than 0.

$$D_1 = a_1 > 0$$

$$D_2 = \begin{vmatrix} a_1 a_3 \\ a_0 a_2 \end{vmatrix} > 0$$

Hurwitz determinant method is lot of time consuming however, Routh has simplified the procedure for ascertaining the number of positive real parts of the roots of polynomial. Therfore, the method is called Routh-Hurwitz criteria.

2. **Nyquist Criterion:** Nyquist criterion is a frequency response method which is used to find out the roots presence in a specified region of s-plane of a characteristic equation. Nyquist criterion is based on open-loop transfer function G(s) H(s). The determination of stability is done from s-plane to G(s) H(s) plane mapping. The independent complex variable is "s" and being the dependent variable G(s) H(s) values are plotted in G(s) H(s) complex plane. In s-plane for every point there is a corresponding point in G(s) H(s) plane.

3. **Bode Plot:** It is a graphical method for determination of the stability on the basis of sinusoidal frequency response. The transfer function for sinusoidal response is obtained by substituting jω in place of the Laplace operator "s" The magnitude and phase angle are expressed for open-loop sinusoidal transfer function G (jω) H (jω). The magnitude of sinusoidal transfer function is expressed in decibel and respective phase angle in degrees with respect to frequency on logarithmic scale in rectangular axis. Thus the plot is known as Bode Plot.

4. **Root Locus:** It is a process of determining the points in s-plane satisfying the following equations:

$$|G(s)H(s)| = 1 \quad \ldots (3.10)$$

$$G(s)H(s) = (2k+1)180^0 \quad \ldots (3.11)$$

The determination of points in s-plane is done by satisfying the equations 3.10 and 3.11. The independent variable is forward path gain K and the roots 1+ G(s) H(s) =0 as dependent variable. With K as variable parameter the roots are plotted in s-plane. From the location of roots in s-plane the system stability and the nature of time response can be ascertained. [6]

Therefore, above are the methods that are used to determine the system stability.

3.4 Control Actions

A control action is used to maintain the output of the system with the desirable limits. The error detector is used to detect output deviations from the reference. The various types of control action used for improving transient and steady state response are described below:

3.4.1 Proportional Control

In actuating signal is proportional to the error signal in the proportional control. The error is the difference of the feedback signal and reference input signal. The system taken under consideration is shown below in figure 3.5:

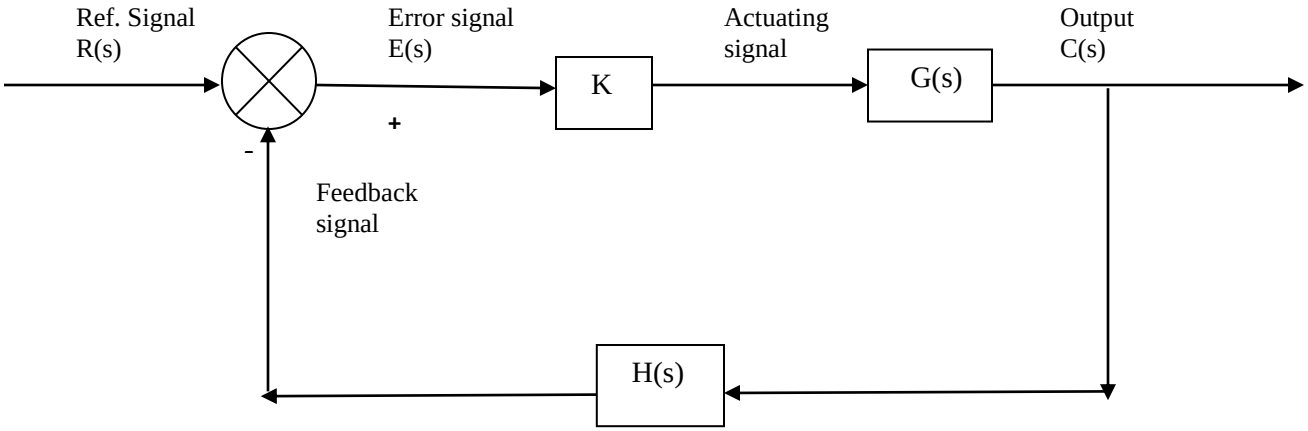

Fig 3.5: Proportional control action

It is desirable that the control system should be underdamped. An underdamped control system exhibits exponentially decaying oscillations during the transient period.

The overdamped response can be made faster by increasing forward path gain of the system. The increase in forward path gain reduces the steady state error and increases the maximum overshoot time.

3.4.2 Derivative control

The actuating signal contains of proportional error added with derivative of the error signal in case of derivative control. For this case, expression of error is given by:

$$e_a(t) = e(t) + T_d \frac{d}{dt} e(t) \quad \ldots (3.12)$$

Where, parameter T_d is a constant

Take the Laplace Transform:

$$E_a(s) = E(s) + s.T_d E(s) \quad \ldots (3.13)$$

The block diagram representation for a second order system with unity feedback is in figure3.6:

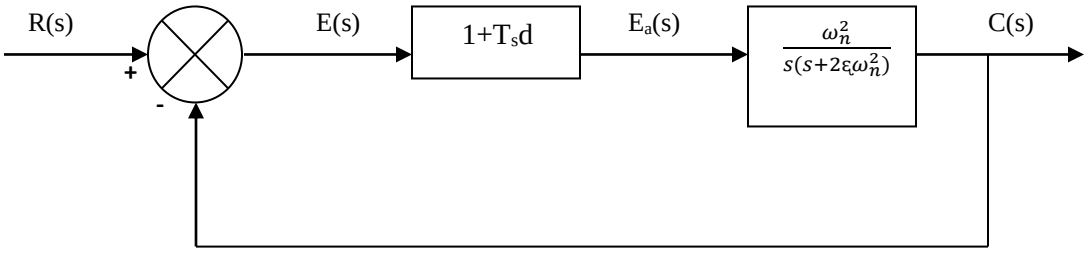

Fig 3.6: Derivative control

The overall transfer function of a second order control system for derivative control is:

$$\frac{C(s)}{R(s)} = \frac{(1+sT_d)\omega_n^2}{s^2+(2\varepsilon\omega_n+\omega_n^2T_d)s+\omega_n^2} \quad \ldots (3.14)$$

Where, ε is a damping ratio and ω_n is a natural frequency

In using derivative control the natural frequency ω_n is unchanged but a zero ($s=-1/T_d$) which results in different expression for time response and the rise time t_r is reduced.

3.4.3 Integral Control

The actuating signal consists of proportional-error signal added with integral of the error signal in integral control. For integral control action the actuating signal is given by:

$$e_a(t) = e(t) + K_t \int e(t)\, dt \quad \ldots (3.15)$$

Where, the parameter K_i is a constant

Take the Laplace Transform of above equation:

$$E_a(s) = E(s) + K_i \frac{E(s)}{s} \quad \ldots (3.16)$$

The block diagram representation using integral control action is given below in figure 3.7:

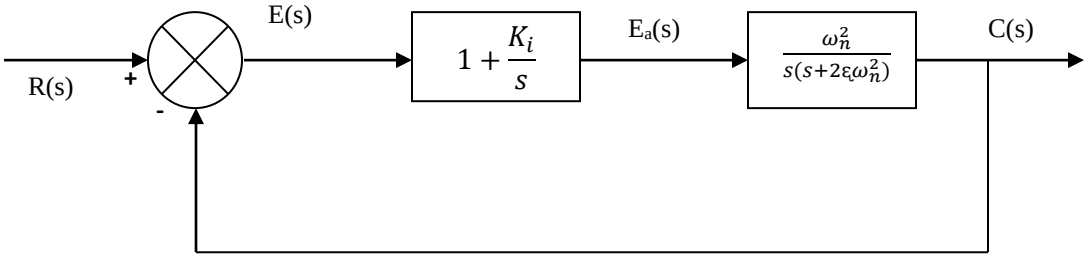

Fig 3.7: Integral control

The transfer function of a closed-loop second order control system using integral control is shown below:

$$\frac{C(s)}{R(s)} = \frac{(s+K_i)\omega_n^2}{s^3+2\varepsilon\omega_n s^2+\omega_n^2 s+K_i\omega_n^2} \quad \ldots (3.17)$$

3.4.4 PID control

In PID control addition with derivative the actuating signal consists of proportional error signal and integral of the error signal. For PID control the actuating signal is:

$$e_a(t) = e(t) + T_d \frac{d}{dt} e(t) + K_i \int e(t)dt \quad \ldots (3.18)$$

Take the Laplace Transform of above equation:

$$E_a(s) = E(s) + sT_dE(s) + \frac{K_i}{s}E(s) \quad \ldots (3.19)$$

The block diagram of a second order control system incorporating PID control is shown below in figure 3.8:

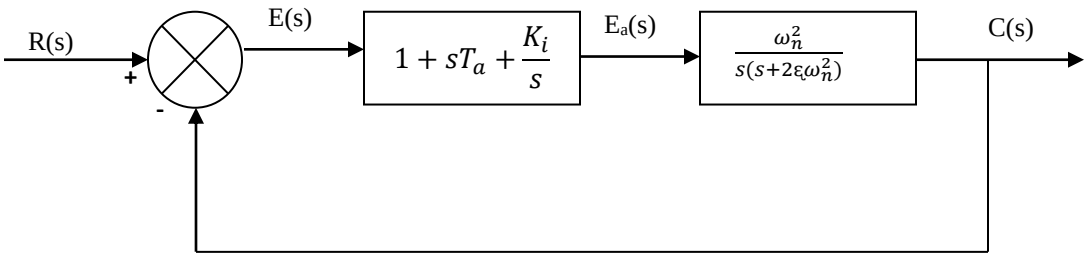

Fig 3.8: PID control

3.5 Method for tuning the gains of the controller

3.5.1 Ziegler-nichols method

For finding the parameters of PID controller various investigation are done on the plant. When the unit step input is applied and there are no conjugate poles and no integrator than the output response is S-shaped. Experimentally such step response curves are generated or by dynamic simulation of the plant. Experimentally to a unit-step input the output of the plant is shown below in figure 3.9: [7]

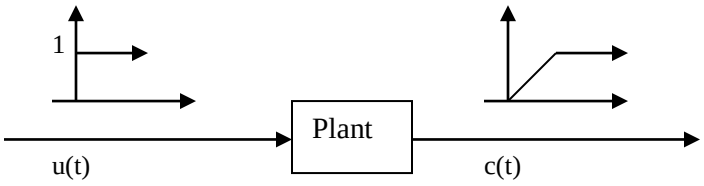

Fig 3.9: Unit step response of a plant

The characterization of S-shaped curve is done by time constant T and delay time L. The determination of these variable constant is done by sketching a tangent line at the curve and determine the intersection of the time axis with the tangent line. The representation of line c(t)= K is done below in figure 3.10:

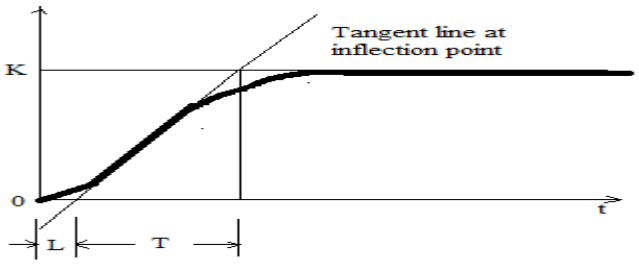

Fig 3.10: S-shaped response

3.5.2 Procedure of tuning the gains of PID controller

The Z-N method is used to operate the gain K_u and T_u the time taken for oscillations for the calculation of K_p. This method of PID controllers tuning is simple and provide better approximations for the controller. The controller constants K_p, K_I, K_d can be obtained for a system with feedback loop. The period of oscillation T_u is the time required when the system at steady-state to complete one full oscillation. The use of K_u and T_u is to find the tuning parameters of the controller. The following procedure is used to calculate the tuning constants:

1. Remove integral and derivative action by setting the integral and derivative gains of the controller to zero value.
2. Increase and decrease the proportional gain until the oscillations attains a constant magnitude.
3. Trace the values of K_u and T_u.
4. Put the values in Z-N expressions and find out the gain of the controller.

The control actions which have been discussed can be used to minimize the error signal for the feedback control and the different characteristics of the output response determine the stability of the system.

CHAPTER 4

Problem Formulation

4.1 Introduction

In power system, if the load is suddenly increased then turbine speed falls as soon as the governor is able to adjust the steam input to adjust the new load. As the governor starts operating the change of speed will result in the minimization of the error. Another way to done the restoration of speed and frequency integrator is applied. For the overcome of the offset integrator is applied which keep a look on the average error. Thus, the uninterrupted changing system load conditions the system generation are repeatedly adjusted for the restoration of the frequency to its actual value. [23] The function of AGC is to maintain the system frequency and the distribution of load among various units of power system for maximum economy.

4.2 AGC in Single Area for linear Governor Characteristics

In the load frequency control loop a modified system load will cause frequency variations, respective to the speed regulation of the governor. In order, to minimize the frequency deviations, we should provide a reset procedure by applying an integrator to change the speed set point by acting on load refrence settings. The integral controller will finally force the frequency variations to zero. The integral controller gains are adjusted such as the transient response is satisfactory. [26] For single area linear governor system as shown in figure 4.1 the block formulation of various components described in Section 2.3.

The closed loop transfer function of the control system is given by:

$$\frac{\Delta f(s)}{-\Delta P_L(s)} = \frac{s(1+T_G s)(1+T_t s)}{s(2Hs+D)(1+T_G s)(1+T_t s)+K_1+\frac{s}{R}} \quad \ldots (4.1)$$

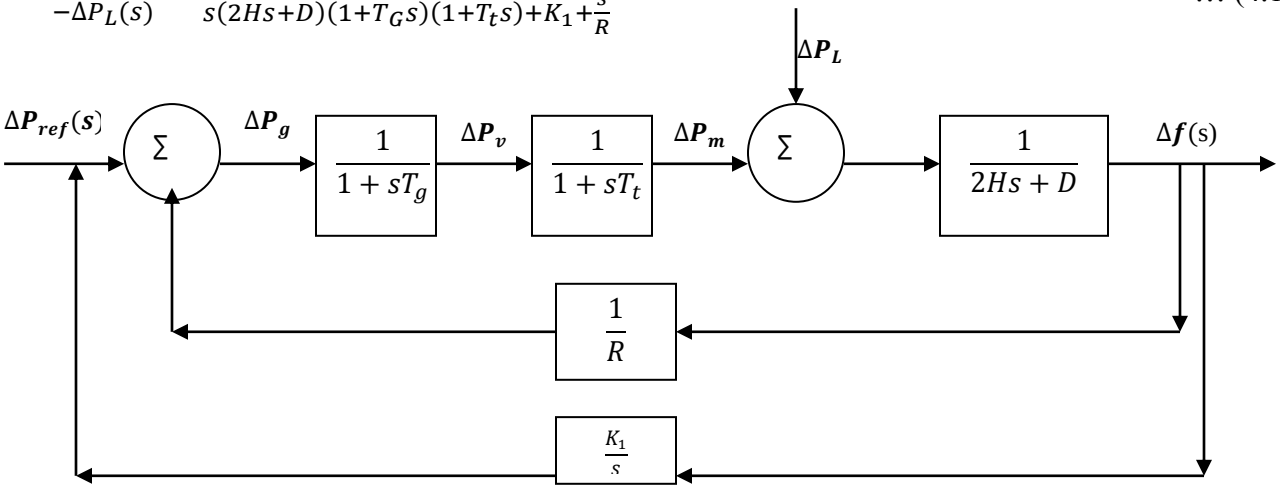

Fig 4.1: Block diagram of AGC in single area

4.3 AGC in Two-Area interconnected system for Linear Governor Characteristics

A two-area interconnected system can be modeled with the help of the assumptions that the each of the interconnected system is replaced by the generating units. The interconnection of these areas is done by the weak lossless line called tie-line. The reactance of this line is considered as X_{12} for representation. For AGC, the transfer function of the tie line power under normal operating conditions is given by: [24]

$$P_{12} = \frac{|E_1||E_2|}{X_{12}} \sin \delta_{12} \quad \ldots (4.2)$$

Where,

E_1, E_2 are the voltages magnitude of interconnected areas 1 and 2.

$$X_{12} = X_1 + X_{tie} + X_2 \quad \ldots (4.3)$$

$$\delta_{12} = \delta_1 - \delta_2 \quad \ldots (4.4)$$

Take small change in angles δ_1 and δ_2 tie line power changes as:

$$\Delta P_{12} = \frac{|E_1||E_2|}{X_{12}} \cos(\delta_1 - \delta_2)(\Delta\delta_1 - \Delta\delta_2) \quad \ldots (4.5)$$

Analogous to the concept of "electrical stiffness" of synchronous machine; we define synchronizing coefficient of a line:

$$T_{12} = \frac{|E_1||E_2|}{X_{12}} \cos(\delta_1 - \delta_2) \text{ Mw/radians} \quad \ldots (4.6)$$

The frequency deviations Δf is related to refrence angle Δ:

$$\Delta f = \frac{1}{2\pi} \frac{d(\delta + \Delta\delta)}{dt} = \frac{1}{2\pi} \frac{d\Delta\delta}{dt} \text{ Hz} \quad \ldots (4.7)$$

Therefore:

$$P_{12} = 2\pi T \left(\int_0^t \Delta f_1 \, dt - \Delta f_2 dt\right) \text{ Mw} \quad \ldots (4.8)$$

The representation of block diagram of tie-line is represented in figure 4.2:

Taking Laplace it yields:

$$\Delta P_{12}(s) = \frac{2\pi T}{s} (\Delta f_1(s) - \Delta f_2(s)) \quad \ldots (4.9)$$

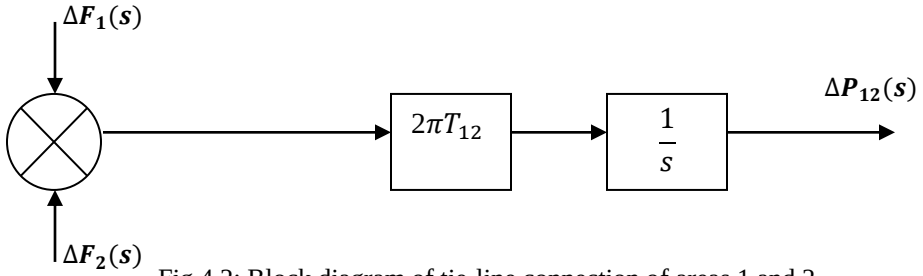

Fig 4.2: Block diagram of tie-line connection of areas 1 and 2

Where,

$$\Delta P_{12} = -\Delta P_{21} \quad \ldots (4.10)$$

Hence, the block diagram of AGC for two-area system as shown in figure 4.3:

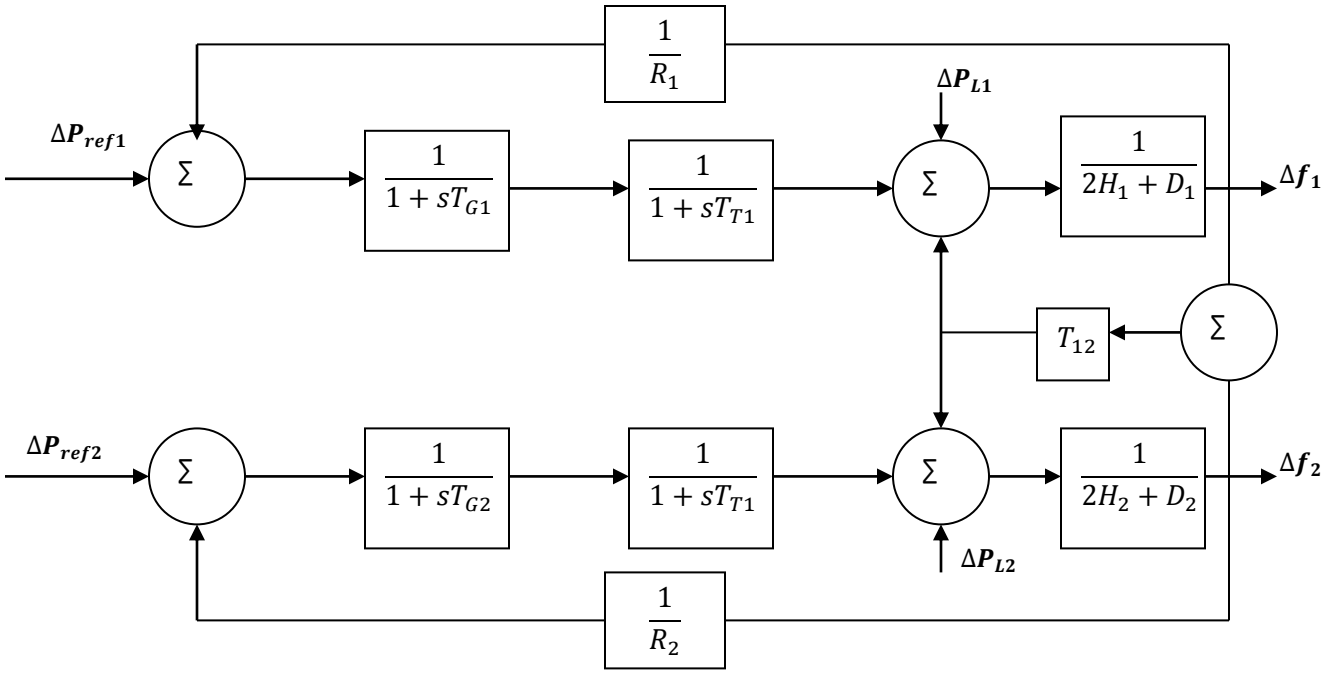

Fig4.3: Two-area system with primary loop LFC

4.4 AGC with non-linear Governor Characteristics

The *transient droop compensation* is required for the governors of the hydraulic units to provide stable speed control performance, therefore it makes the transfer function of hydraulic governor nonlinear. The function of the pressure of water on hydraulic turbine is reduced when a change occur in the gate position of foot of the penstock. Due this change the change in flow does not occur instantly. This is due to the water inertia which temporarily reduces the turbine power. But in the case of deficiency in the generation the deficit of power in hydraulic turbine is more than that of steam turbine. Therfore the initial surge in power occur opposite to the desired. [15] The complete block diagram of hydro turbine-governor system together is shown below in figure 4.4:
It has been seen that the conventional AGC system does not stabilize the hydro turbine-governor system. The reason behind that are the non-linear governor characteristics which make the system unstable. This can also be represented with the help of poles of the system as the positive eigenvalues is the indication of the system unstability. [13]

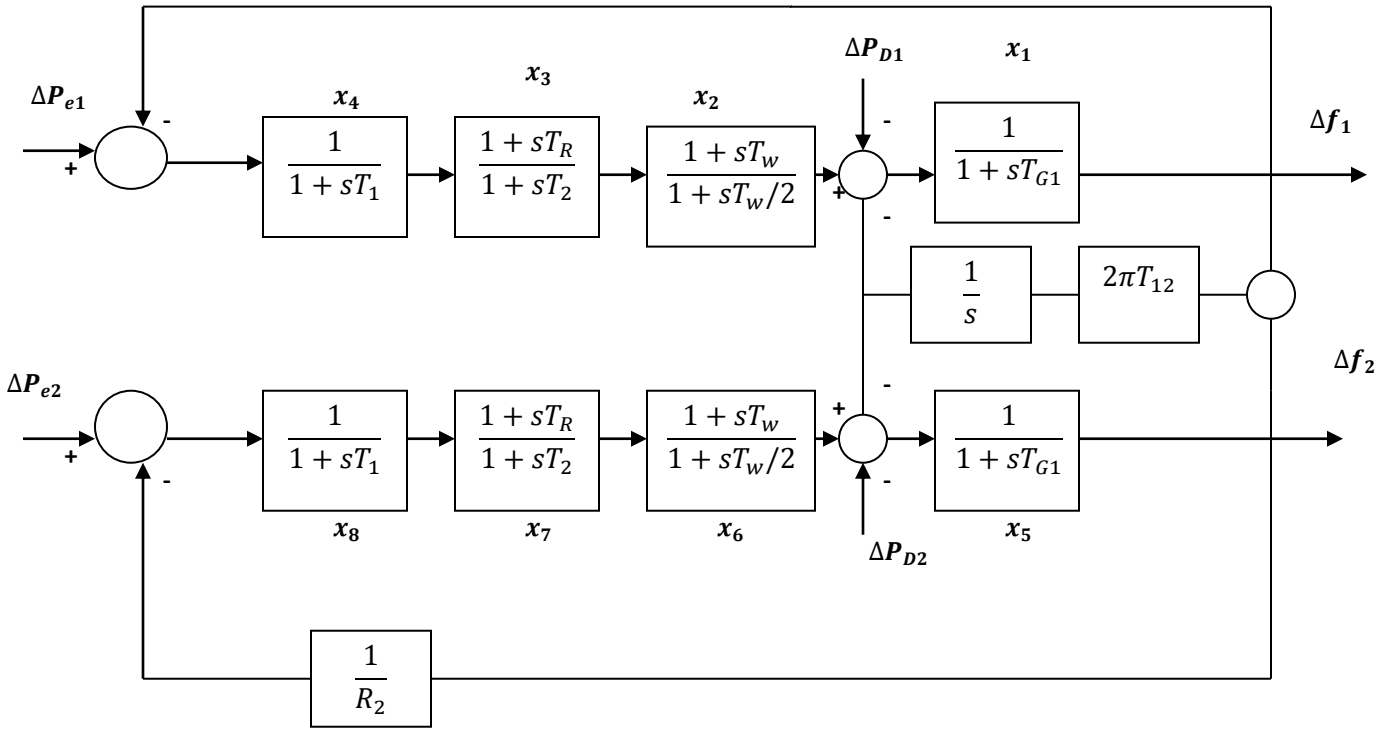

Fig4.4: Block diagram of Two-area hydro turbine-governor system

In order, to find the poles take a test system in Simulink consisting of two units in each area as shown below in figure 4.5:

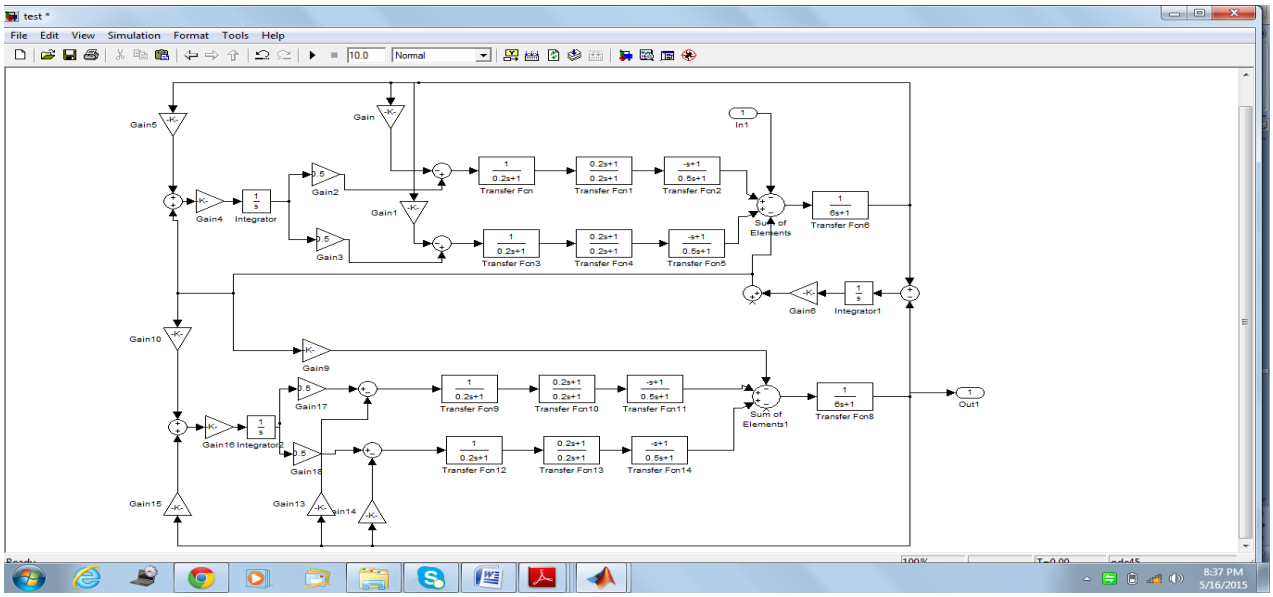

Fig4.5: Snap shot of Test system for two-area hydro-turbine governor system

With reference to the Section 3.3 the stability of system can determined with the help of eigen values of the system. Therefore, the values for the above system are given below:

Sl.No.	Eigen values of test system
1	-4.0422+1.179i
2	-4.0422-1.179i
3	-3.9869+0.9624i
4	-3.9869-0.9624i
5	**0.4613+0.7098i***
6	**0.4613-0.7098i***
7	**0.4062+0.6832i***
8	**0.4062-0.6832i***
9	-5
10	-2
11	-0.0103

When a two-area interconnected network is subjected to 10% load disturbance, system frequency becomes rigorously disturbed and oscillating. The compensation of such sudden load inputs and for the oscillations stabilization, the power flow control of TCPS accompanied with SMES is applied. In order, to overcome the tie-line power oscillations TCPS is applied and for area oscillations compensation SMES is applied. [4] The Linearized model of TCPS and SMES applied to AGC has been discussed in Section 2.3.5.1 and 2.3.5.2. In order to improve the oscillations the complete the model of hydro-hydro system having TCPS and SMES as compensation is shown in the figure below in figure 4.6:

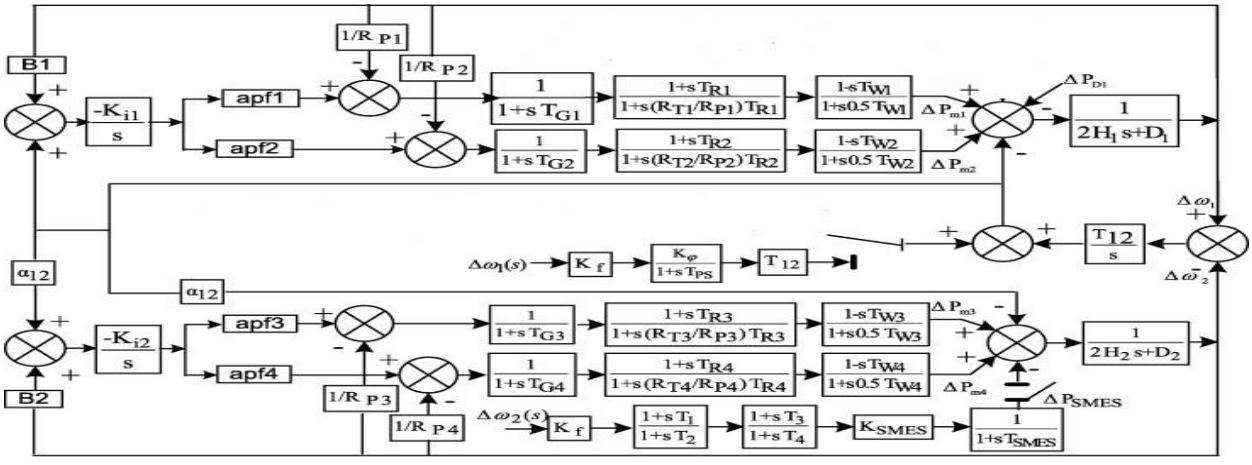

Fig4.6: Linearized model of two-area interconnected hydro-hydro system

Hence the problem has been formulated from the single area system to two-area system for both linear and non-linear governor characteristics. As the hydro-hydro system represent an unstable system which can determined with the help of poles developed from test system as shown above.

CHAPTER 5

Deregulated Environment

5.1 Introduction

The traditional power system consists of VIUs. The VIUs include generating systems, transmission systems and distribution systems. The function is to provide regulated rated power to the customers. The rectangle shaped box represents a VIU in the given figure below. The VIU is associated with different other VIUs and this association occurs at the transmission voltage denoted in the figure 5.1. IPP can also sell power to VIUs which is shown in figure. [13]

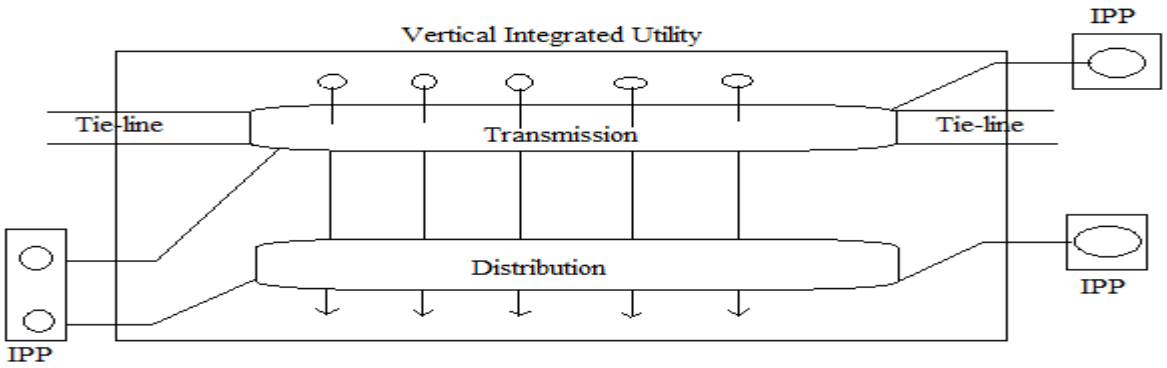

Fig5.1: Vertical Integrated Utility Structure

The existence of vertical integrated utility is no more in deregulated environment. The vertical integrated utility does not have from now onwards generation, transmission and distribution. The deregulated structure consists of many GENCOs and DISCOs, so contract can be occur with GENCO of any area by the DISCO. In another control area also a DISCO may contract with a GENCO. The transactions are named as "bilateral transactions". An independent system operator (ISO) has to be cleared all the transactions. The deregulated structure is shown below in figure 5.2:

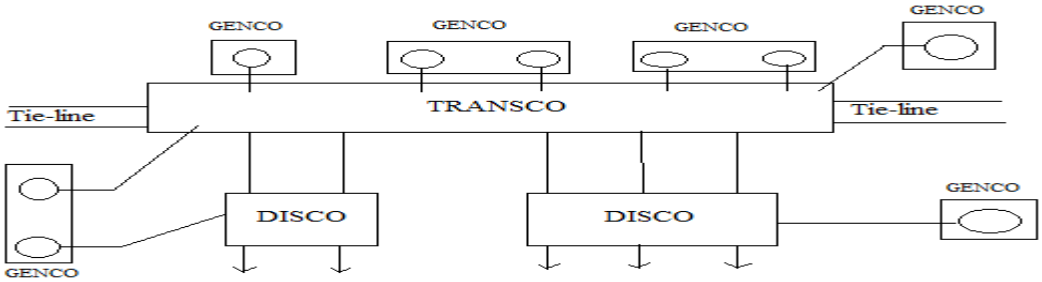

Fig5.2: Deregulated Utility Structure

5.2 AGC in Deregulated Environment

In Deregulated environment, the procedure followed by the AGC is shown in figure 5.3. In this the generating companies send command to Market centre which consists of the bid of regulating reserves. The arrangement and sorting of these biding commands is done by AGC centre on the basis of time and price. Then the AGC centre sends control commands consists of load demanded by DISCO and arranged biding to the generating companies. The re-checking of biding command is continuously done on the basis of information received from tie-line data and the capacity of the GENCO. [11]

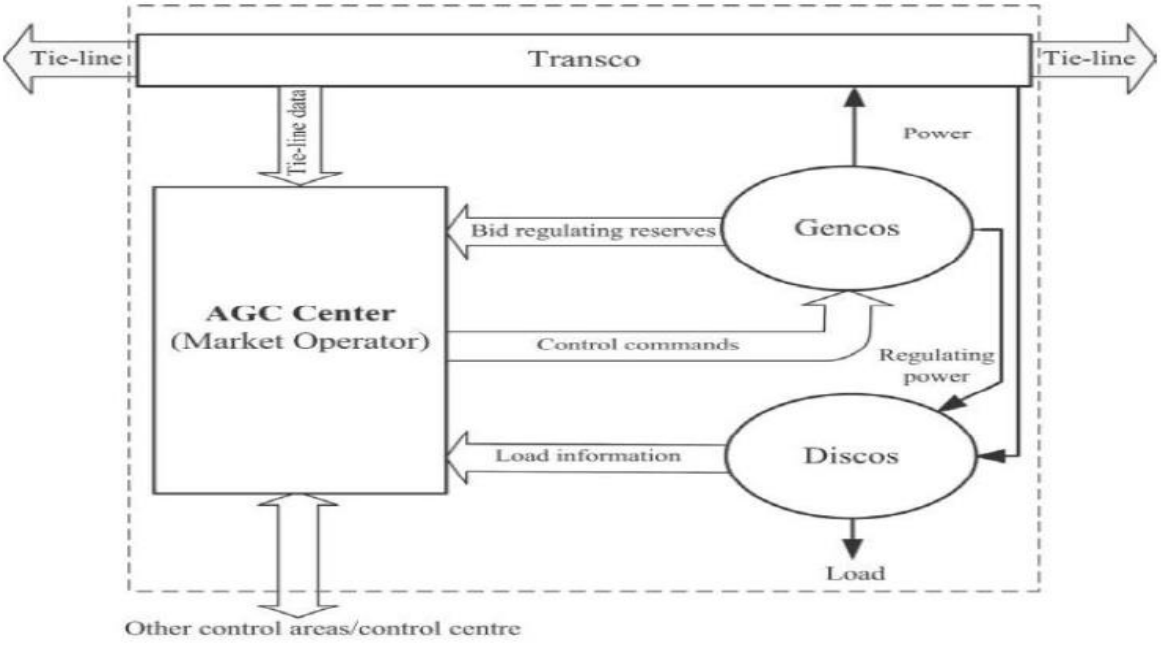

Fig5.3: AGC arrangement in Deregulated Environment

5.3 DPM matrix

In the deregulated environment there is large variation in the prices of transacted power therefore a DISCO can make contract with any GENCO of any area. To carry out these contracts in the mathematical form DISCO participation matrix is introduced in which the rows of this matrix represent the GENCOs and column of this matrix represent DISCO. Suppose if GENCO *i* make a contract with the *j* DISCO then it is represented by the ij^{th} entry in the DISCO participation matrix. The entries given in a column of this matrix should given a sum equal to one. Hence the DISCO participation matrix shows that a number of combinations can be occur between various GENCOs and DISCOs of each area. [13]

Consider a case where a two-area system consists of two GENCOs and two DISCOs in area I and area 2 as shown in figure 5.4:

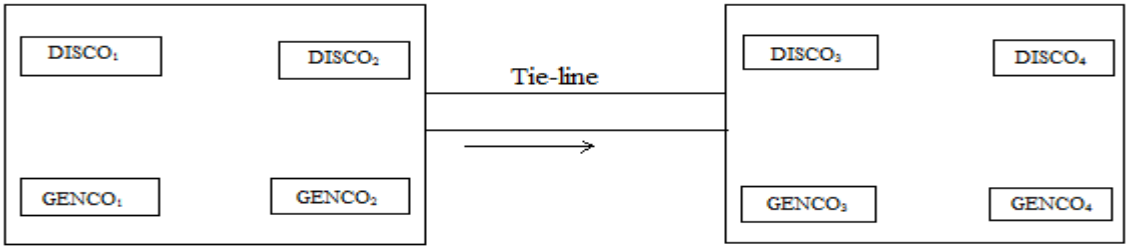

Fig5.4: Two-area system in Deregulated Environment

The corresponding DPM will become,

$$DPM=\begin{bmatrix} cpf_{11} & cpf_{12} & cpf_{13} & cpf_{14} \\ cpf_{21} & cpf_{22} & cpf_{23} & cpf_{24} \\ cpf_{31} & cpf_{32} & cpf_{33} & cpf_{34} \\ cpf_{41} & cpf_{42} & cpf_{43} & cpf_{44} \end{bmatrix}$$

5.4 Formulation of State Model

When the input is provided to the power system corresponding local loads ΔP_{L1} and ΔP_{L2} are represented in each area in the block diagram of deregulated environment. The area control error is distributed among the various areas is based on their participation factor and numbers of GENCOs available. "ACE participation factors" are represented as *apfs* which are distributed to various GENCOs [11]

Where,

$$\sum_{j=1}^{m} apf_j = 1 \quad \ldots (5.1)$$

m is the number of GENCOs

The schedule steady state power flow on the tie lines is given as:

$\Delta P_{\text{tie 1-2 scheduled}}$ = demand (area II DISCOs from area I GENCOs)

\- (area I DISCOs from area IIGENCOs) … (5.2)

$\Delta P_{\text{tie 1-2 error}}$ is defined as,

$$\Delta P_{\text{tie 1-2 error}} = \Delta P_{\text{tie 1-2 actual}} - \Delta P_{\text{tie 1-2 scheduled}} \quad \ldots (5.3)$$

The error signal generates ACE signals for each area.

$$ACE_1 = B_1 \Delta f_1 + \Delta P_{tie1-2\ error} \quad \ldots (5.4)$$

$$ACE_2 = B_2 \Delta f_2 + \Delta P_{tie2-1error} \quad \ldots (5.5)$$

Where,

$$\Delta P_{tie2-1error} = -\frac{p_{r1}}{p_{r2}} \Delta P_{tie1-2error} \quad \ldots (5.6)$$

Where,

P_{r1}, P_{r2} are the rated powers of the given areas,

So,

$$\alpha_{12} = -\frac{p_{r1}}{p_{r2}} \quad \ldots (5.7)$$

The block diagram for AGC in the deregulated environment is shown in the figure 5.5:

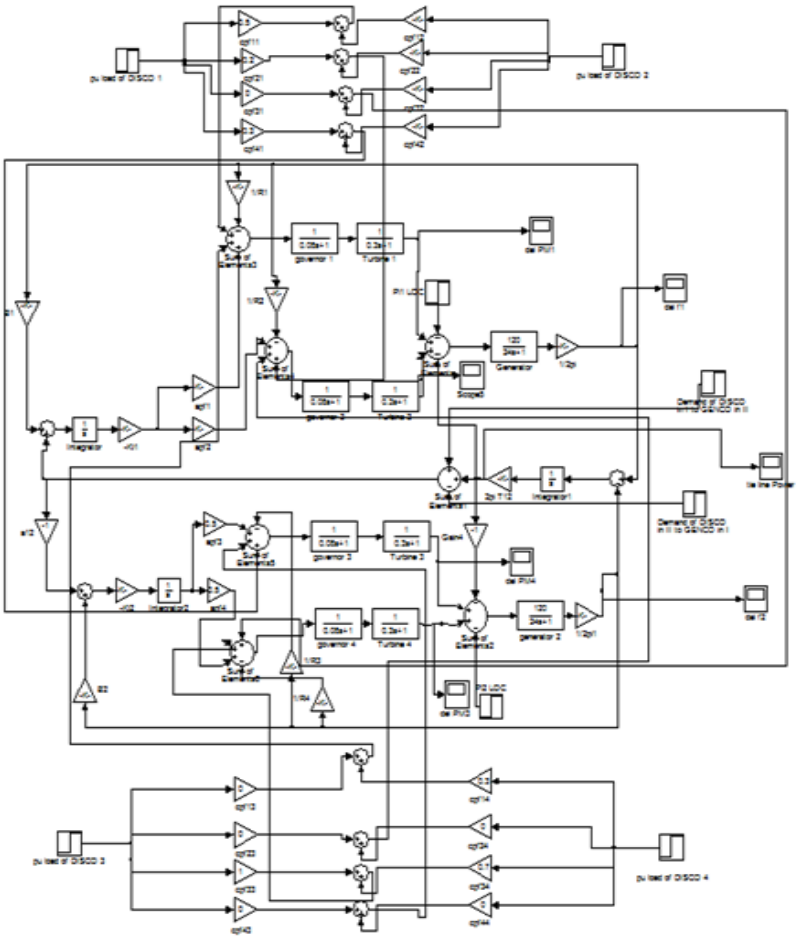

Fig5.5: AGC block diagram in deregulated environment

5.5 State–Space formulation of two-area AGC system with linear Governor Characteristics in Deregulated Environment

The state-space representation of the AGC forms as:

$$\dot{x} = A^{cl}x + B^{cl}u \quad \ldots (5.8)$$

Where,

x represents state vector

u represents vector of power demands of the DISCOs

$$x_1 = \Delta\omega_1 \quad \ldots (5.9)$$

$$x_2 = \Delta\omega_2 \quad \ldots (5.10)$$

$$x_3 = \Delta P_{GV1} \quad \ldots (5.11)$$

$$x_4 = \Delta P_{GV2} \quad \ldots (5.12)$$

$$x_5 = \Delta P_{GV3} \quad \ldots (5.13)$$

$$x_6 = \Delta P_{GV4} \quad \ldots (5.14)$$

$$x_7 = \Delta P_{M1} \quad \ldots (5.15)$$

$$x_8 = \Delta P_{M2} \quad \ldots (5.16)$$

$$x_9 = \Delta P_{M3} \quad \ldots (5.17)$$

$$x_{10} = \Delta P_{M4} \quad \ldots (5.18)$$

$$x_{11} = \int ACE_1 \, dt \quad \ldots (5.19)$$

$$x_{12} = \int ACE_2 \, dt \quad \ldots (5.20)$$

$$x_{13} = \Delta P_{tie1-2} \quad \ldots (5.21)$$

$$x_1 = (\Delta P_{L1,LOC} - x_3 + x_4)\frac{K_{p1}}{1+sT_{p1}} \quad \ldots (5.22)$$

$$\dot{x_1} = \frac{1}{T_{p1}}x_1 - \frac{K_{p1}}{T_{p1}}x_3 + \frac{K_{p1}}{T_{p1}}x_4\Delta P_{L1,LOC} \quad \ldots (5.23)$$

$$x_2 = (\Delta P_{L2,LOC} - \alpha_{12}x_3 + x_6)\frac{K_{p2}}{1+sT_{p2}} \quad \ldots (5.24)$$

$$\dot{x_2} = \frac{1}{T_{p2}}x_1 - \alpha_{12}\frac{K_{p2}}{T_{p2}}x_3 + \frac{K_{p2}}{T_{p2}}x_6 - \Delta P_{L1,LOC}\frac{K_{p2}}{T_{p2}} \quad \ldots (5.25)$$

$$x_3 = \frac{1}{1+sT_{T1}}x_4 \quad \ldots (5.26)$$

$$\dot{x_3} = \frac{1}{T_{T1}}(x_4 - x_3) \quad \ldots (5.27)$$

$$x_4 = \frac{1}{1+sT_{T2}}x_5 \quad \ldots (5.28)$$

$$\dot{x_4} = \frac{1}{T_{T2}}(x_5 - x_4) \quad \ldots (5.29)$$

$$x_5 = \frac{1}{1+sT_{T3}}x_6 \quad \ldots (5.30)$$

$$\dot{x_5} = \frac{1}{T_{T3}}(x_6 - x_5) \quad \ldots (5.31)$$

$$x_6 = \frac{1}{1+sT_{T4}}x_7 \quad \ldots (5.32)$$

$$\dot{x_6} = \frac{1}{T_{T4}}(x_7 - x_6) \quad \ldots (5.33)$$

$$\dot{x_7} = -\frac{x_1}{T_{G1}R_1} - \frac{x_5}{T_{G1}} + (-K_1 apf_1)\frac{1}{T_{G1}} \quad \ldots (5.34)$$

$$\dot{x_8} = -\frac{x_1}{T_{G2}R_2} - \frac{x_6}{T_{G2}} + (-K_1 apf_2)\frac{1}{T_{G2}} \quad \ldots (5.35)$$

$$\dot{x_9} = -\frac{x_2}{T_{G3}R_2} - \frac{x_7}{T_{G3}} + (-K_2 apf_3)\frac{1}{T_{G3}} \quad \ldots (5.36)$$

$$\dot{x_{10}} = -\frac{x_2}{T_{G4}R_2} - \frac{x_8}{T_{G4}} + (-K_2 apf_4)\frac{1}{T_{G4}} \quad \ldots (5.37)$$

$$\dot{x_{11}} = B_1 x_1 + x_{13} \quad \ldots (5.38)$$

$$\dot{x_{12}} = B_2 x_2 + \alpha_{12} x_{13} \quad \ldots (5.39)$$

$$\dot{x_{13}} = \frac{T_{12}}{2\pi}(x_1 - x_2) \quad \ldots (5.40)$$

The equations in matrix form written as [13]:

A^{cl}	1	2	3	4	5	6	7	8	9	10	11	12	13
1	$-1/T_{P1}$	0	K_{P1} $/T_{P1}$	K_{P1} $/T_{P1}$	0	0	0	0	0	0	0	0	$-K_{P1}$ $/T_{P1}$
2	0	-1 $/T_{P2}$	0	0	K_{P2} $/T_{P2}$	K_{P2} $/T_{P2}$	0	0	0	0	0	0	K_{P2} $/T_{P2}$
3	0	0	-1 $/T_{T1}$	0	0	0	1 $/T_{T1}$	0	0	0	0	0	0
4	0	0	0	-1 $/T_{T2}$	0	0	0	1 $/T_{T2}$	0	0	0	0	0
5	0	0	0	0	-1 $/T_{T3}$	0	0	0	1 $/T_{T3}$	0	0	0	0
6	0	0	0	0	0	-1 $/T_{T4}$	0	0	0	1 $/T_{T4}$	0	0	0
7	-1 $/2\pi R_1 T_{G1}$	0	0	0	0	0	-1 $/T_{G1}$	0	0	0	$-K_1$ apf_1/T_{G1}	0	0
8	-1 $/2\pi R_2 T_{G2}$	0	0	0	0	0	0	-1 $/T_{G2}$	0	0	$-K_1 apf_2$ $/T_{G2}$	0	0
9	0	-1 $/2\pi T_{G3} R_3$	0	0	0	0	0	0	-1 $/T_{G3}$	0	0	$-K_2$ apf_3 $/T_{G3}$	
10	0	1 $/2\pi R_4 T_{G4}$	0	0	0	0	0	0	0	-1 $/T_{G4}$	0	$-K_2$ apf_4 $/T_{G4}$	0
11	$B_1/2\pi$	0	0	0	0	0	0	0	0	0	0	0	1
12	0	$B_2/2\pi$	0	0	0	0	0	0	0	0	0	0	-1

13	$T_{12}/2\pi$	$-T_{12}/2\pi$	0	0	0	0	0	0	0	0	0	0	0

B^{cl}	1	2	3	4
1	$-K_{P1}/T_{P1}$	$-K_{P1}/T_{P1}$	0	0
2	0	0	$-K_{P2}/T_{P2}$	$-K_{P2}/T_{P2}$
3	0	0	0	0
4	0	0	0	0
5	0	0	0	0
6	0	0	0	0
7	cpf_{11}/T_{G1}	cpf_{12}/T_{G1}	cpf_{13}/T_{G1}	cpf_{14}/T_{G1}
8	cpf_{21}/T_{G2}	cpf_{22}/T_{G2}	cpf_{23}/T_{G2}	cpf_{24}/T_{G2}
9	cpf_{31}/T_{G3}	cpf_{32}/T_{G3}	cpf_{33}/T_{G3}	cpf_{34}/T_{G3}
10	cpf_{41}/T_{G4}	cpf_{42}/T_{G4}	cpf_{43}/T_{G4}	cpf_{44}/T_{G4}
11	cpf_{31}/cpf_{41}	$cpf_{32}+cpf_{42}$	$-(cpf_{13}+cpf_{23})$	$-(cpf_{14}+cpf_{24})$
12	$-(cpf_{31}+cpf_{41})$	$-(cpf_{32}+cpf_{42})$	$cpf_{13}+cpf_{23}$	$cpf_{14}+cpf_{24}$
13	0	0	0	0

$u= [\Delta P_{L1}\ \Delta P_{L2}\ \Delta P_{L3}\ \Delta P_{L4}]^{T}$

$x= [\Delta\omega_1\ \Delta\omega_2\ \Delta P_{GV1}\ \Delta P_{GV2}\ \Delta P_{GV3}\ \Delta P_{GV4}\ \Delta P_{M1}\ \Delta P_{M2}\ \Delta P_{M3}\ \Delta P_{M4} \int ACE_1\,dt \int ACE_2\,dt\ \Delta P_{tie1\text{-}2}]$

On substituting the System Data given in the Appendix I we get the vector matrices A^{cl} and B^{cl} values as shown below:

A^{cl}	1	2	3	4	5	6	7	8	9	10	11	12	13
1	-0.0416	0	5	5	0	0	0	0	0	0	0	0	-5
2	0	-0.0416	0	0	5	5	0	0	0	0	0	0	5
3	0	0	-3.33	0	0	0	3.33	0	0	0	0	0	0
4	0	0	0	-3.33	0	0	0	3.33	0	0	0	0	0
5	0	0	0	0	-3.33	0	0	0	3.33	0	0	0	0
6	0	0	0	0	0	-3.33	0	0	0	3.33	0	0	0
7	-0.829	0	0	0	0	0	-12.5	0	0	0	-0.242	0	0
8	-0.829	0	0	0	0	0	0	-12.5	0	0	-0.242	0	0

9	0	-0.829	0	0	0	0	0	0	-12.5	0	0	-0.087	0
10	0	-0.829	0	0	0	0	0	0	0	-12.5	0	-0.087	0
11	0.067	0	0	0	0	0	0	0	0	0	0	0	1
12	0	0.067	0	0	0	0	0	0	0	0	0	0	-1
13	0.086	-0.086	0	0	0	0	0	0	0	0	0	0	0

B^{cl}	1	2	3	4
1	-5	5	0	0
2	0	0	-5	-5
3	0	0	0	0
4	0	0	0	0
5	0	0	0	0
6	0	0	0	0
7	0.04	0.04	0	0
8	0.04	0.04	0	0
9	0	0	0	0
10	0	0	0	0
11	0	0	0	0
12	0	0	0	0
13	0	0	0	0

5.6 State-Space formulation with non-linear Governor Characteristics in Deregulated Environment

The state-space representation of AGC forms as:

$$\dot{x} = A^{cl}x + B^{cl}u \quad \ldots (5.41)$$

Where,

x represents as state vector

u represents vector of power demands of the DISCOs

$$x_1 = \Delta\omega_1 \quad \ldots (5.42)$$

$$x_2 = \Delta\omega_2 \quad \ldots (5.43)$$

$$\dot{x_1} = -\frac{1}{T_{ps1}}x_1 + \frac{K_{ps1}}{T_{ps1}}x_2 - \frac{K_{ps1}}{T_{ps1}}\Delta P_{D1} - \frac{K_{ps1}}{T_{ps1}}\Delta P_{tie} \quad \ldots (5.44)$$

$$\dot{x_2} = -\frac{x_2}{0.5T_w} + x_3\left(\frac{1}{0.5T_w} + \frac{1}{0.5T_2}\right) - \frac{x_4}{0.5}\left(\frac{1}{T_2} - \frac{T_R}{T_{G1}T_2}\right) - \frac{T_R}{0.5T_{G1}T_2}\Delta P_{e1} + \frac{T_R}{0.5R_{p1}T_{G1}T_2}x_1 \quad \ldots (5.45)$$

$$\dot{x_3} = -\frac{x_3}{T_2} + x_4\left(\frac{1}{T_2} - \frac{T_R}{T_{G1}T_2}\right) + \frac{T_R}{T_{G1}T_2}\Delta P_{e1} - \frac{T_R}{R_{p1}T_{G1}T_2}x_1 \quad \ldots (5.46)$$

$$\dot{x_4} = -\frac{1}{T_{G1}}x_4 - \frac{1}{T_{G1}R_{p1}}x_1 + \frac{1}{T_{G1}}\Delta P_{e1} \quad \ldots (5.47)$$

$$\dot{x_5} = -\frac{1}{T_{ps2}}x_5 + \frac{K_{ps2}}{T_{ps2}}x_6 - \frac{K_{ps2}}{T_{ps2}}\Delta P_{D2} + \frac{K_{ps2}}{T_{ps2}}\Delta P_{tie} \quad \ldots (5.48)$$

$$\dot{x_6} = -\frac{x_6}{0.5T_w} + x_7\left(\frac{1}{0.5T_w} + \frac{1}{0.5T_2}\right) - \frac{x_8}{0.5}\left(\frac{1}{T_2} - \frac{T_R}{T_{G2}T_2}\right) - \frac{T_R}{0.5T_{G2}T_2}\Delta P_{e2} + \frac{T_R}{0.5R_{p2}T_1T_2}x_5 \quad \ldots (5.49)$$

$$\dot{x_7} = -\frac{x_7}{T_2} + x_8\left(\frac{1}{T_2} - \frac{T_R}{T_{G2}T_2}\right) + \frac{T_R}{T_{G2}T_2}\Delta P_{e2} - \frac{T_R}{R_{p2}T_{G2}T_2}x_5 \quad \ldots (5.50)$$

$$\dot{x_8} = -\frac{1}{T_{G2}}x_8 - \frac{1}{T_{G2}R_{p2}}x_5 + \frac{1}{T_{G2}}\Delta P_{e2} \quad \ldots (5.51)$$

$$\dot{x_9} = 2\pi T_{12}(x_1 - x_5) \quad \ldots (5.52)$$

These equations in matrix form written as:

A^{cl}	1	2	3	4	5	6	7	8	9
1	-1 /T_{ps1}	-K_{ps1} /T_{ps1}	0	0	0	0	0	0	-K_{ps1} /T_{ps1}
2	T_R/ 0.5$Rp_1T_{G1}T_2$	-1 /0.5T_w	(1/0.5T_w) +(1/0.5T_2)	-1/0.5 (1/T_2- T_R/$T_{G1}T_2$)	0	0	0	0	0
3	-T_R/ $R_{p1}T_{G1}T_2$	0	-1/T_2	1/T_2- T_R/$T_{G1}T_2$	0	0	0	0	0
4	-1/$T_{G1}R_{p2}$	0	0	-1/T_{G1}	0	0	0	0	0
5	0	0	0	0	-1/T_{ps2}	K_{ps2}/T_{ps2}	0	0	K_{ps2}/T_{ps2}
6	0	0	0	0	T_R /0.5$R_{p2}T_{G2}T_2$	-1 /0.5T_w	1/0.5T_w +1/0.5T_2	- 1/0.5(1/T_2 - T_R/$T_{G2}T_2$)	0
7	0	0	0	0	-T_R/ $R_{p2}T_{G2}T_2$	0	-1/T_2	1/T_2- T_R/$T_{G2}T_2$	0
8	0	0	0	0	-1/$T_{G2}R_{p2}$	0	0	-1/T_{G2}	0
9	2πT_{12}	0	0	0	-2πT_{12}	0	0	0	0

[x] = [Δf_1 ΔP_{m1} ΔP_{GV1} ΔX_{e1} Δf_2 ΔP_{m2} ΔP_{GV2} ΔX_{e2} ΔP_{tie}]

B^{cl}	1	2
1	0	0
2	$-T_R/0.5T_{G1}T_2$	0
3	$T_R/T_{G1}T_2$	0
4	$1/T_{G1}$	0
5	0	0
6	0	$-T_R/0.5T_{G2}T_2$
7	0	$T_R/T_{G2}T_2$
8	0	$1/T_{G2}$
9	0	0

$[u] = [\Delta P_{e1}\ \Delta P_{e2}]$

On substituting the System Data given in the Appendix I we get the vector matrices A^{cl} and B^{cl} are shown below:

A^{cl}	1	2	3	4	5	6	7	8	9
1	-8.33	-8.33	0	0	0	0	0	0	-8.33
2	200	-2	12	0	0	0	0	0	0
3	-100	0	-5	0	0	0	0	0	0
4	-100	0	0	-5	0	0	0	0	0
5	0	0	0	0	-8.33	8.33	0	0	8.33
6	0	0	0	0	200	-2	12	0	0
7	0	0	0	0	-100	0	-5	0	0
8	0	0	0	0	-100	0	0	-5	0
9	0.543	0	0	0	-0.543	0	0	0	0

B^{cl}	1	2
1	0	0
2	-10	0
3	5	0
4	5	0
5	0	0

6	0	-10
7	0	5
8	0	5
9	0	0

5.7 Evaluation of two-area system in Deregulated Environment under different Scenarios

5.7.1 Scenario 1: Base Case (same apfs)

In this case GENCOs in each area equally participate which is represented by the apfs i.e. [16] [18]

apf_1 =0.5

apf_2 =0.5

apf_3 =0.5

apf_4 =0.5

The load contracted by each area is taken as 0.1. Therefore, the DPM matrix for this case becomes.

$$DPM = \begin{bmatrix} 0.5 & 0.5 & 0 & 0 \\ 0.5 & 0.5 & 0 & 0 \\ 0 & 0 & 0 & 0 \\ 0 & 0 & 0 & 0 \end{bmatrix}$$

It shows that the GENCOs of the area I are participating equally, however the GENCOs of area II does not contract any load thus represented by zero.

The generation of GENCOs in p.u MW can be represents as contract participation factor and DISCOs demand as:

$$\Delta P_{Mi} = cpf_{ij}\Delta P_{Lj} \quad \ldots (5.53)$$

Where,

Therefore in this case,

$$\Delta P_{Mi} = cpf_{i1}\Delta P_{L1} + cpf_{i2}\Delta P_{L2} + cpf_{i3}\Delta P_{L3} + cpf_{i4}\Delta P_{L4} \quad \ldots (5.54)$$

Therefore, we have,

$\Delta P_{M1} = 0.5 * \Delta P_{L1} + 0.5 * \Delta P_{L2}$ =0.1 p.u. MW

And accordingly,

ΔP_{M2} =0.1 p.u. MW

ΔP_{M3} =0 p.u. MW

ΔP_{M4} =0 p.u. MW

The steady-state generated power of $GENCO_3$ and $GENCO_4$ are zero which shows that it does not contract any load demand from any DISCO. The optimized values of the controllers tuned by Ziegler-nichols are given in Table 3 and Table 4 and Genetic Algorithm tuned values for both linear and non-linear governor characteristics are given in Section 7.2.4.1.

5.7.2 Scenario 2: Different apfs

In this case all DISCOs of each area make contract with all the GENCOs of each area. Therefore, the DPM becomes:

$$\text{DPM} = \begin{bmatrix} 0.5 & 0.25 & 0 & 0.3 \\ 0.2 & 0.25 & 0 & 0 \\ 0 & 0.25 & 1 & 0.7 \\ 0.3 & 0.25 & 0 & 0 \end{bmatrix}$$

The area participation factor of the above case is given as following, where the DISCO of the each area demand loads of 0.1:

apf_1 =0.75

apf_2 =0.25

apf_3 =0.5

apf_4 =0.5

The off diagonal parameters of the DPM represents that DISCO in one area make contract with a GENCO of another area.

$$\Delta P_{tie1-2scheduled} = \sum_{i=1}^{2}\sum_{j=3}^{4} cpf_{ij}\,\Delta P_{Lj} - \sum_{i=3}^{4}\sum_{j=1}^{2} cpf_{ij}\,\Delta P_{Lj} \quad \ldots (5.55)$$

Hence,

$\Delta P_{tie1\text{-}2scheduled}$ =-0.05 p.u. MW

The respective optimized of the controller tuned with Ziegler-nichols, when trajectories reach the desired values are given in Table 5 and Table 6 and Genetic Algorithm tuned values for both linear and non-linear characteristics are given in Section 7.2.4.2.

5.7.3 Scenario 3: Contract violation

The demand more power by the DISCO than that specified in the contract violates the contract, and then any GENCO does not contract this excess power. The GENCOs in the same areas as the DISCO this uncontracted power must be supplied. It must be reflected not as the contract demand but as the local load of the area. The DPM is given in case 2: [3]

$\Delta P_{L1,\,LOC}$ (local load area I)

$= (0.1+0.1) + 0.1 = 0.3$ p.uMW … (5.56)

Similarly, $\Delta P_{L2,\ LOC}$

= 0.2 p.uMW (no uncontracted load) … (5.57)

In the case of the uncontracted load, the area in which this uncontracted load appears only that area will take this excess load that is $GENCO_1$, however the generation of all areas that is $GENCO_3$ and $GENCO_4$ remains unaffected. In all other areas except $GENCO_1$ the load is distributed on the basis of the area participation factor of this case.

The respective optimized values of the controller tuned with Ziegler-nichols, when trajectories reach the desired values are given in Table 7 and Table 8 and Genetic Algorithm tuned values are given in Section 7.2.4.3.

Due to the changing market trends it important to study deregulated environment considering the AGC role. Therefore the system has been modeled according to deregulated environment for both linear and non-linear governor characteristics and various cases has been developed due to the different types of transactions involved.

CHAPTER 6

Solution Methodology

6.1 Introduction

The genetic operation is based on Darwinian Survival of the fittest principal which is popularly known as Genetic Algorithm. This method is effective for optimization. This global optimization technique involves stochastic search algorithm. Since the gains of the controller are to be optimized using GA, binary strings are assigned to each member of the population. The accommodation of the entire range of possible solutions is done by selecting large value of population size. GA implementation starts with parameter encoding. This has to be done effectively so that the link in the objective function and the strings is properly maintained. [12]

6.1.1 Terminology

The important terminologies to which Genetic algorithm is associated with are: [8]

(i) Individual: An individual referred to as any point at which the application of objective function is done. With these variables the optimization of the objective function is going to be done. The objective function value is given the name called its score. It is also named as a genome and vector.

(ii) Population: It is referred to as an array of individuals. If the population size is 50 and in the objective function number of variables is 3, each row represents an individual in the population of a 50 by 3 matrix.

(iii) Generation: At each iterations, the genetic algorithm performs computation on the new population by applying genetic operators in order to produce a new population. Each successive set of population is known as a new generation.

(iv) Parents and Children: To create the next population genetic algorithm select individuals in the current population which are called parents, and further new individuals which are called children are created in next generation. In next generation children are obtained from parents by applying following genetic operators:

1 Reproduction: The current population fittest children are selected and transferred in next population. The children given the name called Elite children.

2 Cross-over: This operator is used to exchange genetic information of individual pairs with one another. The children having the name called Crossover children.

3 Mutations: This operator follows some Probabilistic Rule and change genetic representation. The children given the name called Mutation children.

(v) Decimal to Binary string formulation

The decimal integers of binary strings can be obtained as follows,

$$y_j = \sum_{i=1}^{l} 2^{i-1} b_{ij} \; (j = 1,2, \ldots \ldots, L) \quad \ldots (6.1)$$

Where,

y_{ij} is the decimal coded value of the binary string

b_{ij} is the ith binary digit of the jth string

l is the length of the string

L is the population size

(vi) Mapping

Following a fixed mapping rule, the continuous variable x_j is found in the search space where x_{min} and x_{max} are the minimum and maximum values of the variable x_j.

Where,

$$x_j = x_{min} + \frac{x_{max} - x_{min}}{2^l - 1} \quad \ldots (6.2)$$

The evaluation of best values of controller gains is obtained to minimize the objective function. This task ensures small overshoot, fast rise time and quick settling time.

(vii) Probability

The probability of selecting the ith string is,

$$p_i = \frac{f_i}{\sum_{j=1}^{L} f_j} \quad \ldots (6.3)$$

Where,

f_i is the fitness of ith population

The fitness function is used to rank and for the allocation of reproductive series in the Genetic Algorithm. This means that the reproductive unit which has higher rank is being selected as a parent.

6.1.2 Algorithm

With the above description and reference to the various genetic parameters given in Appendix II, the steps of applied genetic algorithm for the tested system are given below:

Step1: Set the values of generation counter (gen_count), mutation rate (bitmut), population size (n), population counter (r), maximum (min) and minimum values (max) of variables, string size (p) etc.

Step 2: Code the variables of the problem into binary strings according to the equation (6.1).

Step 3: Using random number generation (rand) create the initial population having random values lies between 0 and 1. If the value is greater than 0.5 consider it 0 otherwise consider it 1.

Step 4: Initialize the generation counter (gen_count).

Step 5: Initialize the population counter (r) and increase the generation counter (gen_count).

Step 6: Decode the binary strings (d) given in equ. (6.2) and increase the population counter (r).

Step 7: Use these values of variables (k_i) in Simulink model in order to find out the objective function given in Section 7.2.

Step 8: Check the fitness function (fitness)

where, $fitness = \frac{1}{ACE}$.

Step 9: If the population counter (r) is less than the size of population (n), GOTO step 4 and repeat.

Step 10: The highly fit strings are selected as parents and offspring are produced by allocating number of copies to each individual according to their fitness by using probability equation 6.3.

Step 11: Generate new strings using crossover by mating current offspring with a random generated template (temp). This is done by generating a random number and compared it with crossover probability Pc. If it is less than Pc performs crossover otherwise retain the string.

Step 12: Introduce variations in the strings by mutation operator (bitmut) and the existing strings are replaced by new strings (new_pop). This is done by generating a random number and compared it with mutation probability Pm. If it is less than Pm performs mutation otherwise retain the string.

Step 13: Check if the generation counter (gen_count) is less than the iteration number. If true, GOTO step 5 and repeat. Otherwise

Step 14: Stop

The flow chart of the above process is given below:

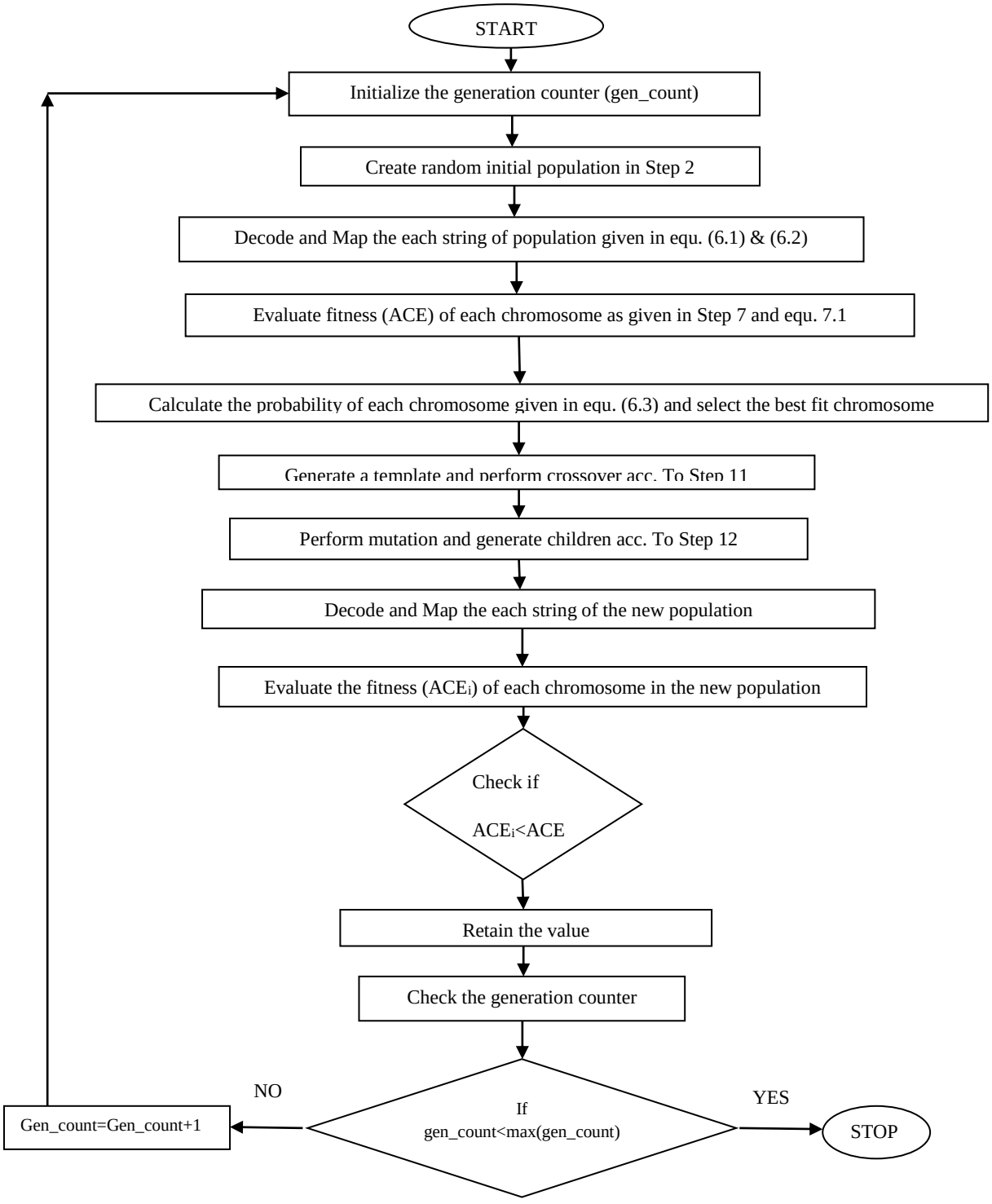

Fig6.1: Flow chart of Genetic algorithm

Hence Genetic algorithm is used for tuning the gains of the controller in order to stabilize the system frequency oscillations.

CHAPTER 7
SIMULATION RESULTS

7.1 Simulation results with Ziegler-nichols technique

7.1.1 Test Case 1: Simulation results of two-area system with linear governor characteristics

With reference to the Block diagram of two-area interconnected system in the figure 4.3 when implemented with feedback control whose gains are optimized by Ziegler-nichols method following optimal values are obtained:

TABLE 7.1: Ziegler-nichols based gains of two-area with linear governor

Ziegler-nichols based optimal values			
Control Areas	K_p	K_i	K_D
Area-1	0.3	0.15	0.15
Area-2	0.2	0.1	0.0125
K_{u1}	0.50		
K_{u2}	0.33		
T_u	4 sec		

TABLE 7.2: Ziegler-nichols based time response parameters of two-area with linear governor

Parameters	Undershoot	Settling time	Rise time	Delay time
Δf_1	-0.165	40 sec	1.5 sec	1.15 sec
Δf_2	-0.125	42 sec	2 sec	1.65 sec

7.1.2 Test Case 2: Simulation results of two-area system in Deregulated Environment with Ziegler-nichols method

With reference to the block diagram of two-area interconnected system in deregulated environment given in the figure 5.5 when implemented with Ziegler-nichols method following optimized values of gains is obtained in various Scenarios.

7.1.2.1 Scenario 1: Base Case (same apfs)

According to the discussion given in the Section 5.7.1 the optimized values of the controller for linear governor characteristics are given below:

TABLE 7.3: Ziegler-nichols based gains of two-area with linear governor in deregulated environment (with same apfs)

Ziegler-nichols based optimal values			
Control Areas	K_p	K_i	K_D
Area-1	0.1	0.067	0.0375
Area-2	0.05	0.033	0.0187
K_{u1}	0.166		
K_{u2}	0.083		
T_u	3 sec		

TABLE 7.4: Ziegler-nichols based time response parameters of two-area with linear governor in deregulated environment (with same apfs)

Parameters	Overshoot	Undershoot	Settling time	Rise time	Delay time
Δf_1	0.0135	-0.0376	35 sec	1.5 sec	1.2 sec
Δf_2	0.0124	-0.035	30 sec	2.4 sec	1.7 sec
Tie-line	0.048	-0.0625	35 sec	1.88 sec	1.4 sec

7.1.2.2 Scenario 2: Different apfs

According to the discussion given in the Section 5.7.2 the optimized values of the controller for linear governor characteristics are given below:

TABLE 7.5: Ziegler-nichols based gains of two-area with linear governor in Deregulated Environment (with different apfs)

Ziegler-nichols based optimal values			
Control Areas	K_p	K_i	K_D
Area-1	0.2	0.1	0.1
Area-2	0.1	0.05	0.05
K_{u1}	0.33		
K_{u2}	0.167		
T_u	4 sec		

TABLE 7.6: Ziegler-nichols based time response parameters of two-area with linear governor in deregulated environment (with different apfs)

Parameters	Overshoot	Undershoot	Settling time	Rise time	Delay time
Δf_1	0.007	-0.058	30 sec	1.8 sec	1.2 sec
Δf_2	0.004	-0.036	25 sec	1.5 sec	1.1 sec
Tie-line	0.001	-0.075	30 sec	2.5 sec	2 sec

7.1.2.3 Scenario 3: Contract violation

According to the discussion given in the Section 5.7.3 the optimized values of the controller for linear governor characteristics are given below:

TABLE 7.7: Ziegler-nichols based gains of two-area with linear governor in deregulated environment (with contract violation)

Ziegler-nichols based optimal values			
Control Areas	K_p	K_i	K_D
Area-1	0.1	0.05	0.05
Area-2	0.1	0.05	0.05
K_{u1}	0.167		
K_{u2}	0.167		
T_u	4 sec		

TABLE 7.8: Ziegler-nichols based time response parameters of two-area with linear governor in deregulated environment (with contract violation)

Parameters	Overshoot	Undershoot	Settling time	Rise time	Delay time
Δf_1	0.01	-0.08	25 sec	1.6 sec	1.2 sec
Δf_2	0.04	-0.04	30 sec	2.6 sec	1.15 sec
Tie-line	0.01	-0.12	30 sec	2.4 sec	1.7 sec

7.2 Simulation results with Genetic Algorithm

7.2.1 Problem Formulation

The objective is to minimize the performance index which is the integral square error of two-area interconnected system is represented below. For the relation between various parameters given below refer to the equations given in Section 5.5.

Minimize $J = \int \sum_{i=1}^{m} (ACE_i^2)$ … (7.1)

Where, m is the number of control areas in the system

Area control errors are given as:

$ACE_1 = B_1 \Delta f_1 + \Delta P_{tie1-2error}$ … (7.2)

$ACE_2 = B_2 \Delta f_2 - \Delta P_{tie1-2error}$ … (7.3)

Where,

$ACE_{1,2}$ =Area control error

B_1, B_2 =Bias factor

Δf_1, Δf_2 =incremental change in frequency of area 1 and area 2

$\Delta P_{tie1\text{-}2error}$ =incremental change in tie-line power

Where,

$\Delta P_{tie1-2error} = \Delta P_{tie1-2actual} - \Delta P_{tie1-2scheduled}$ … (7.4)

Subjected to,

$K_{p,i}^{min} \leq K_{p,i} \leq K_{p,i}^{max}$

$K_{I,i}^{min} \leq K_{I,i} \leq K_{I,i}^{max}$

$K_{D,i}^{min} \leq K_{D,i} \leq K_{D,i}^{max}$

Where,

$K_{p,i}$, $K_{I,i}$, $K_{D,i}$ are the proportional, integral and derivative gains of the PID controller of the i^{th} area, $K_{p,i}^{min}$, $K_{I,i}^{min}$, $K_{D,i}^{min}$ and $K_{p,i}^{max}$, $K_{I.i}^{max}$, $K_{D,i}^{max}$ are the lower bound and upper bound of the PID controller parameters. Further to satisfy the requirement of non-linear governor system parameters of TCPS (K_φ, T_{ps}), parameters of SMES (K_{SMES}, T_{SMES}, T_1, T_2, T_3, T_4) are also to be optimized.

7.2.2 Test Case 3: Simulation results of two-area system with linear governor characteristics

With reference to the block diagram of two-area interconnected system as shown in the figure 4.3, the gains are controlled by genetic algorithm. The following optimized gains are provided:

TABLE 7.9: Genetic Algorithm based gains of two-area with linear governor

Genetic Algorithm based optimal values				
Control Areas	Integral Controller	PID controller		
	K_i	K_p	K_i	K_D
Area-1	0.3085	0.5804	0.3912	0.7442
Area-2	0.2449	0.5850	0.4153	0.7595

TABLE 7.10: Genetic Algorithm based time response parameters of two-area with linear governor

Parameters	Overshoot	Undershoot	Settling time	Rise time	Delay time
With integral controller					
Δf_1	0.040	-0.21	25 sec	1.8 sec	1.1 sec
Δf_2	0.038	-0.16	20 sec	1.4 sec	1 sec
With PID controller					
Δf_1	0.001	-0.075	18 sec	1.3 sec	1 sec
Δf_2	0.004	-0.045	15 sec	2 sec	1.5 sec

TABLE 7.11: Output response of genetic algorithm based two-area with linear governor

Parameters	**Integral**	**PID**
Δf_1	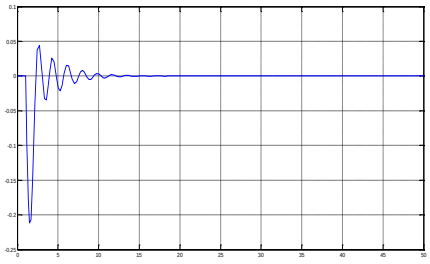	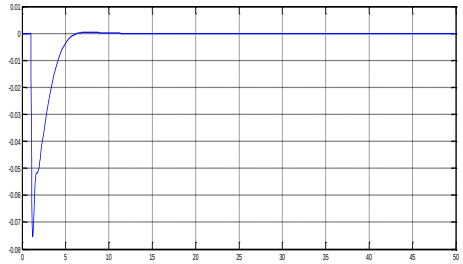
Δf_2	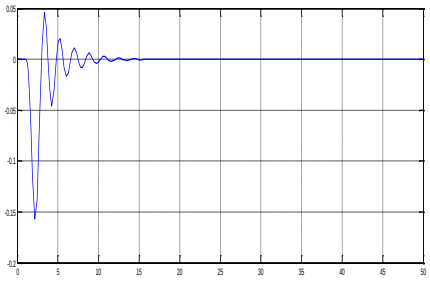	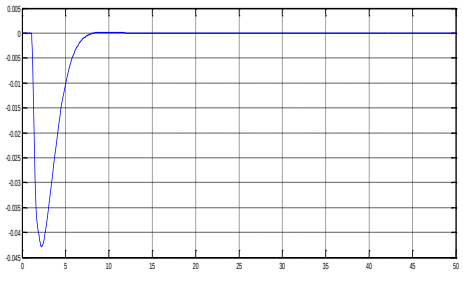

7.2.3 Test Case 4: Simulation results of two-area system with non-linear governor characteristics

With reference to the block diagram of two-area interconnected system as shown in the figure 4.4, the gains are controlled by genetic algorithm. The following optimized gains are provided:

TABLE 7.12: Genetic Algorithm based gains of two-area with non-linear governor

TCPS-SMES coordination with Integral Controller					
Area 1					
K_φ		T_{ps}		K_{i1}	
0.2857		0.3601		0.0431	
Area 2					
K_{SMES}	T_1	T_2	T_3	T_4	K_{i2}
0.3886	0.1	0.0303	0.1745	0.1076	0.0780

TCPS-SMES coordination with PID controller							
Area 1							
K_φ		T_{ps}		K_p	K_I	K_D	
0.3012		0.1864		0.0852	0.0509	0.0178	
Area 2							
K_{SMES}	T_1	T_2	T_3	T_4	K_p	K_I	K_D
0.2134	0.1510	0.1248	0.1752	0.1167	0.0417	0.0485	0.0265

TABLE 7.13: Genetic Algorithm based time response parameters of two-area with non-linear governor

Parameters	Overshoot	Undershoot	Settling time	Rise time	Delay time
With integral controller					
Δf_1	0.016	-0.03	70 sec	5 sec	3.62 sec
Δf_2	0.015	-0.025	55 sec	4.6 sec	2.69 sec
With PID controller					
Δf_1	0.009	-0.12	65 sec	4.8 sec	3.3sec
Δf_2	0.005	-0.15	60 sec	3.2 sec	2.5 sec

TABLE 7.14: Output response of genetic algorithm based two-area with non-linear governor

Parameters	Integral	PID
Δf_1	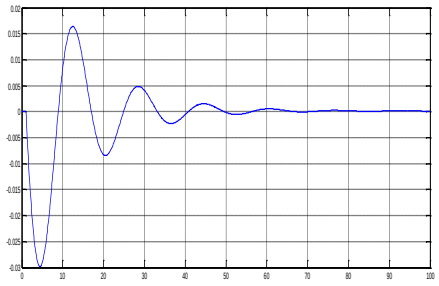	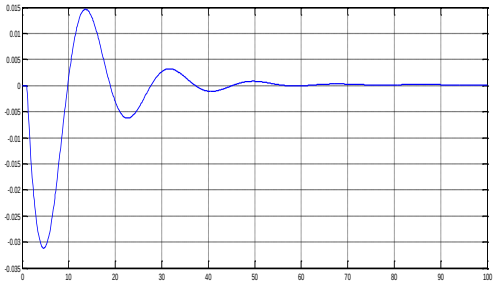
Δf_2	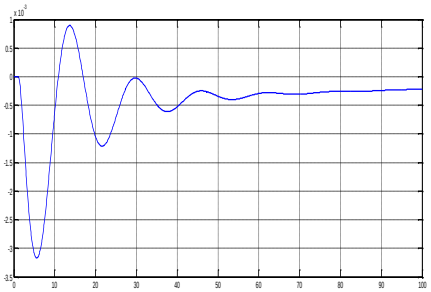	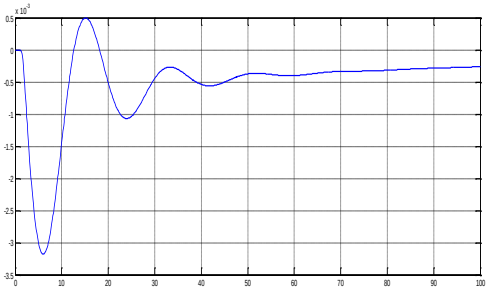

7.2.4 Test Case 5: Simulation results of two-area system in Deregulated Environment

The simulation results of two-area system in Deregulated Environment have been plotted with the use of Integral (I) and Proportional Integral Derivative Controller (PID). The system data related to the block diagram parameters of linear and non-linear governor characteristics is used for simulation. Both areas are assumed to be identical. The governor-turbine units in each area are assumed to be identical.

7.2.4.1 Scenario 1: Base Case (same apfs)

According to the Base case discussed in the Section 5.7.1 the results of the load change: area frequency deviations, actual power flow on the tie-line and the generated powers of the various GENCOs following a step change in load demand of $DISCO_1$ and $DISCO_2$ for linear and non-linear governor characteristics are shown below:

TABLE 7.15: Output response of genetic algorithm based two-area with linear governor in Deregulated Environment (with same apfs)

Parameters	Linear Governor (Integral)	Linear Governor (PID)
Δf_1	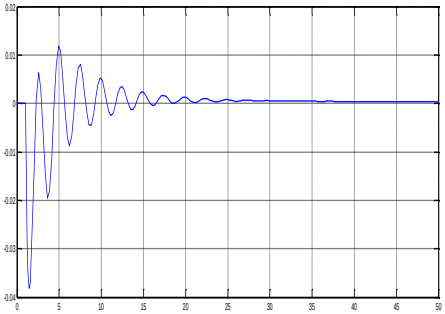	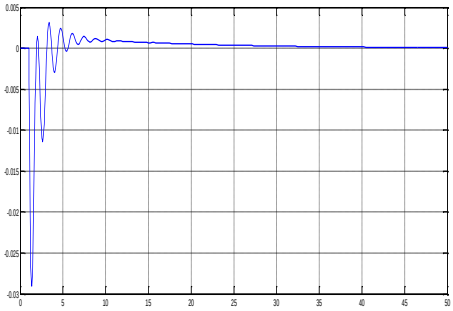
Δf_2	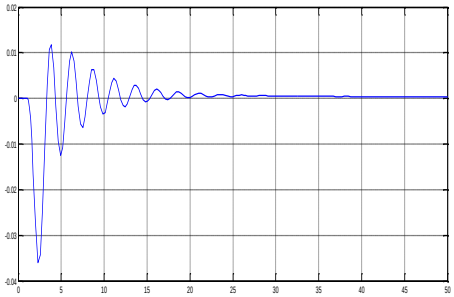	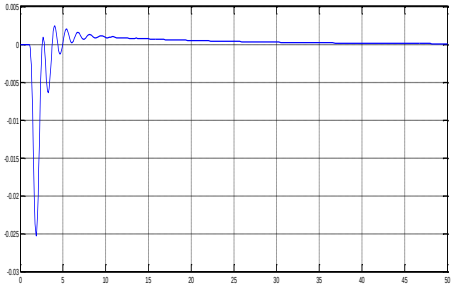
Tie-line	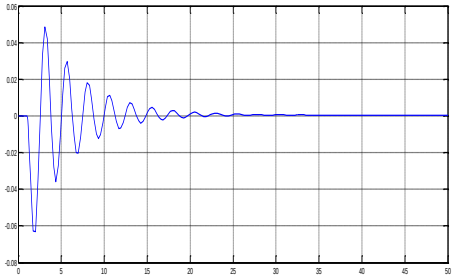	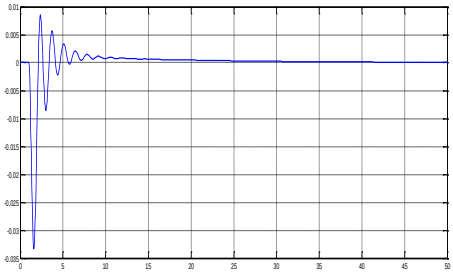
GENCO1	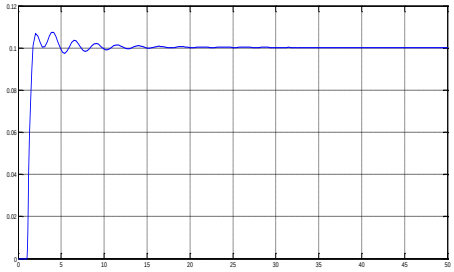	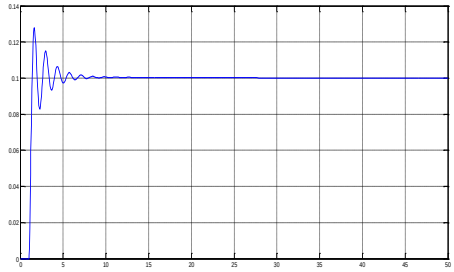

GENCO2	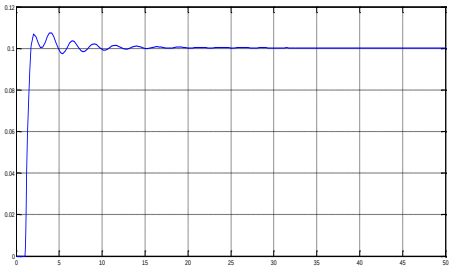	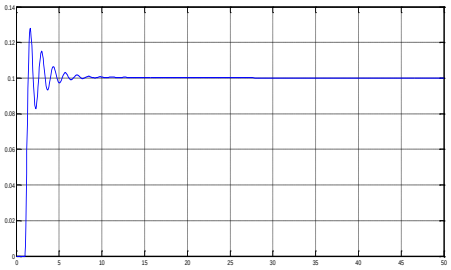
GENCO3	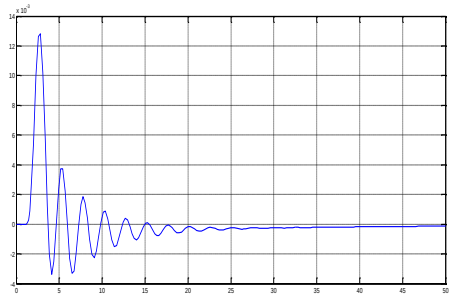	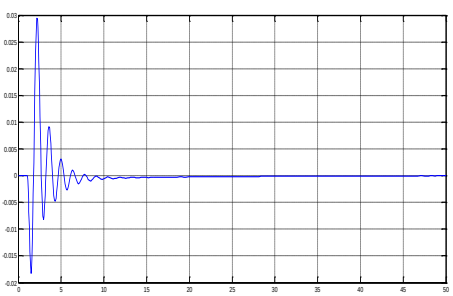
GENCO4	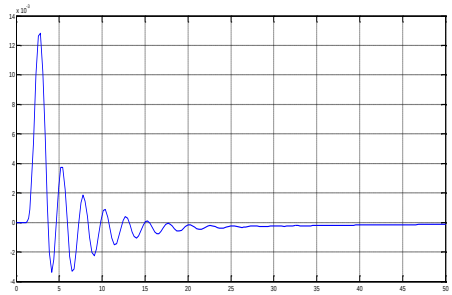	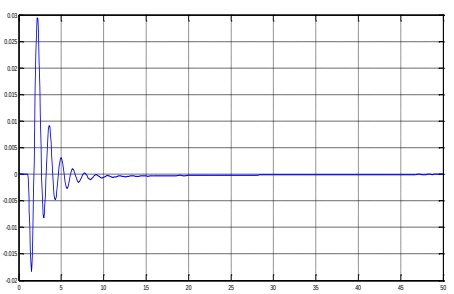

TABLE 7.16: Output response of genetic algorithm based two-area with non-linear governor in Deregulated Environment (with same apfs)

Parameters	**Non-linear Governor (integral)**	**Non-linear Governor (PID)**
Δf_1	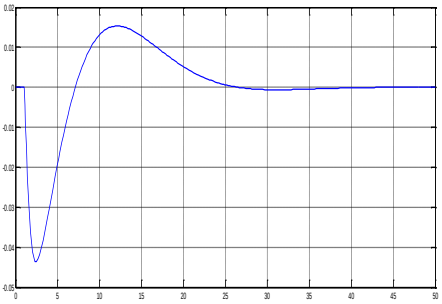	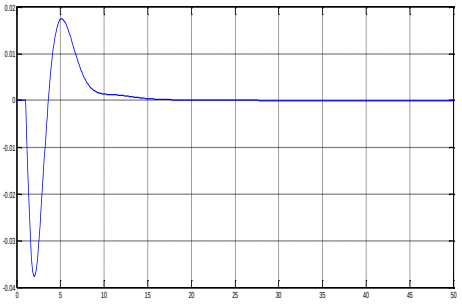

Δf_2	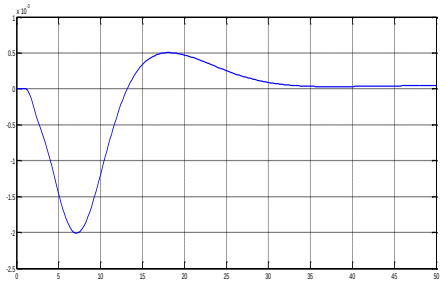	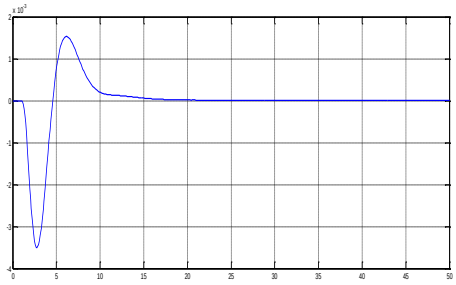
Tie-line	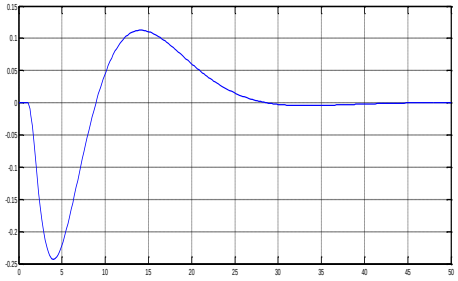	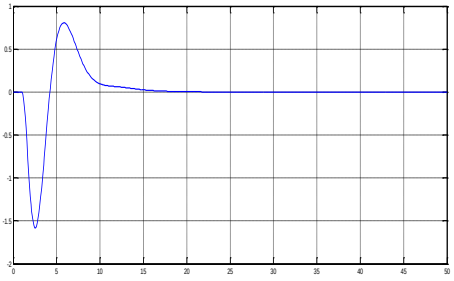
GENCO1	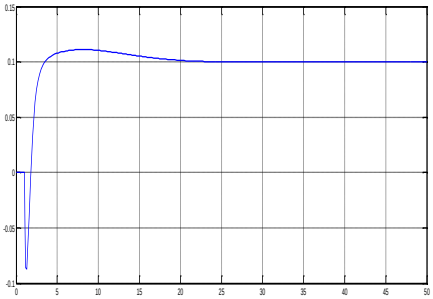	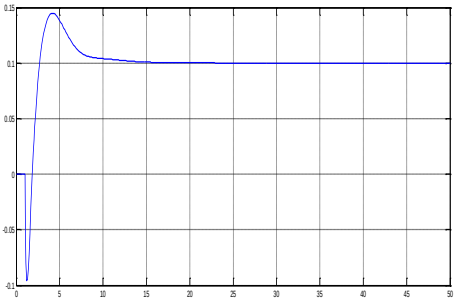
GENCO2	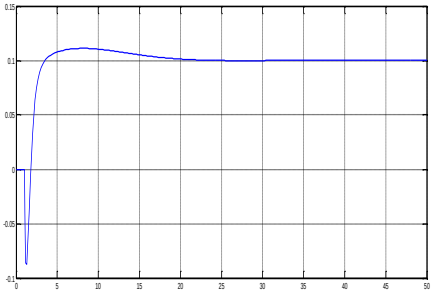	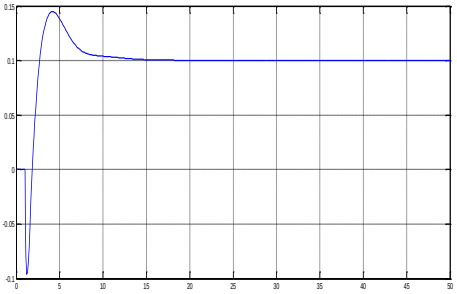

GENCO3	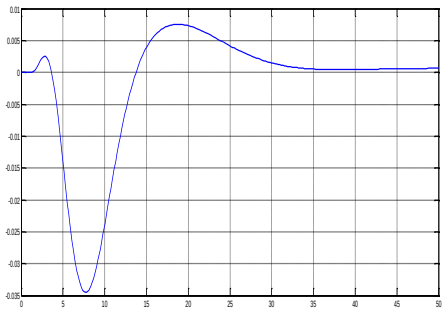	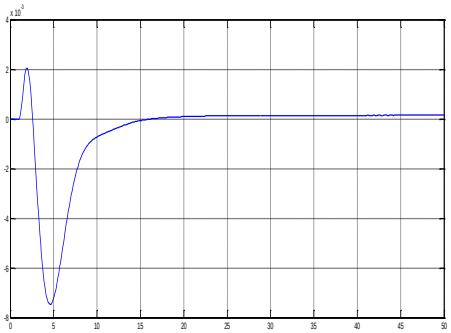
GENCO4	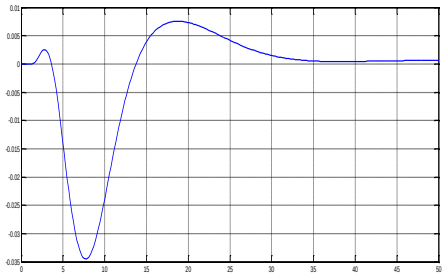	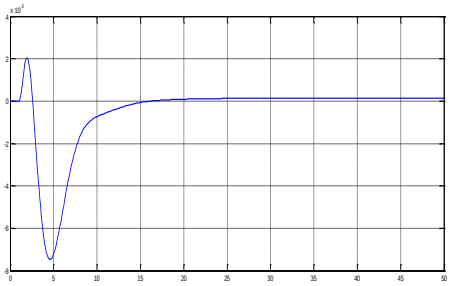

TABLE 7.17: Genetic Algorithm based gains of two-area with linear governor in Deregulated Environment (with same apfs)

Genetic Algorithm based optimal values				
Control Areas	Integral Controller	PID controller		
	K_i	K_p	K_i	K_D
Area-1	0.1388	0.3572	0.2593	0.4662
Area-2	0.2140	0.2586	0.3514	0.4044

TABLE 7.18: Genetic Algorithm based time response parameters of two-area with linear governor in Deregulated Environment (with same apfs)

Parameters	Overshoot	Undershoot	Settling time	Rise time	Delay time
With integral controller					
Δf_1	0.012	-0.038	25 sec	1.42 sec	1.14 sec
Δf_2	0.011	-0.036	30 sec	2.3 sec	1.5 sec
Tie-line	0.048	-0.05	30 sec	2 sec	1.4 sec

With PID controller					
Δf_1	0.005	-0.029	12 sec	1.35 sec	1 sec
Δf_2	0.002	-0.025	10 sec	2 sec	1.6 sec
Tie-line	0.008	-0.033	15 sec	1.69 sec	1.3 sec

TABLE 7.19: Genetic Algorithm based gains of two-area with non-linear governor in Deregulated Environment (with same apfs)

TCPS-SMES coordination with Integral Controller					
Area 1					
K_φ		T_{ps}		K_{i1}	
0.2414		0.1067		0.0295	
Area 2					
K_{SMES}	T_1	T_2	T_3	T_4	K_{i2}
0.8869	0.0846	0.0778	0.1764	0.1554	0.2490

TCPS-SMES coordination with PID controller							
Area 1							
K_φ		T_{ps}		K_p	K_I	K_D	
0.0863		0.1211		0.0487	0.0105	0.0469	
Area 2							
K_{SMES}	T_1	T_2	T_3	T_4	K_p	K_I	K_D
0.2189	0.1876	0.0615	0.0796	0.0986	0.0143	0.0210	0.0149

TABLE 7.20: Genetic Algorithm based time response parameters of two-area with non-linear governor in Deregulated Environment (with same apfs)

Parameters	Overshoot	Undershoot	Settling time	Rise time	Delay time
With integral controller					
Δf_1	0.0153	-0.0435	35 sec	2.5 sec	1.36 sec
Δf_2	0.005	-0.002	40 sec	4.8 sec	2.5 sec
Tie-line	0.1125	-0.243	40 sec	4 sec	2 sec

With PID controller					
Δf_1	0.0175	-0.0377	15 sec	2 sec	1.3 sec
Δf_2	0.0015	-0.035	20 sec	4 sec	2 sec
Tie-line	0.6	-0.016	20 sec	2.2 sec	1.5 sec

7.2.4.2 Scenario 2: Different apfs

According to the Case 2 discussed in the Section 5.7.2 the results of the load change: area frequency deviations, actual power flow on the tie-line and the generated powers of the various GENCOs following a step change in load demand of $DISCO_1$ and $DISCO_2$ for linear and non-linear governor characteristics are shown below:

TABLE 7.21: Output response of genetic algorithm based two-area with linear governor in Deregulated Environment (with different apfs)

Parameters	**Linear Governor (Integral)**	**Linear Governor (PID)**
Δf_1	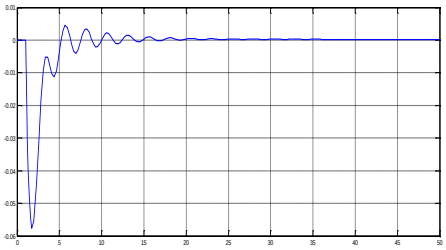	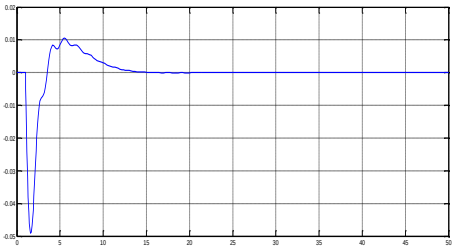
Δf_2	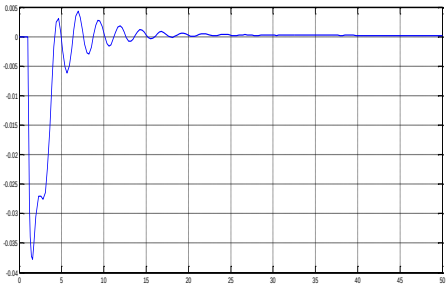	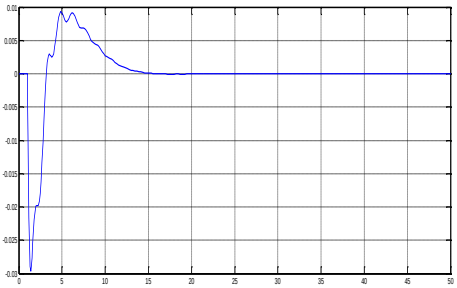
Tie-line	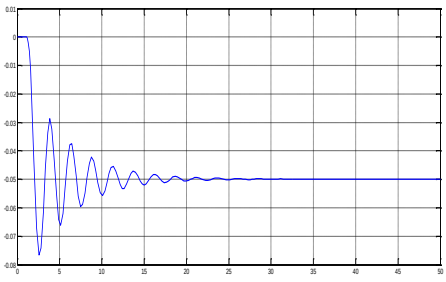	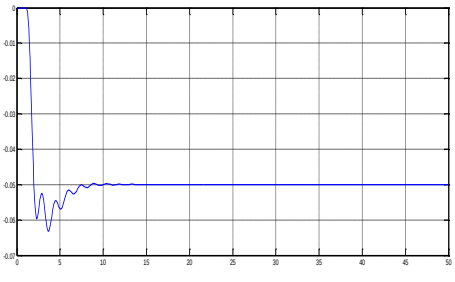

GENCO1	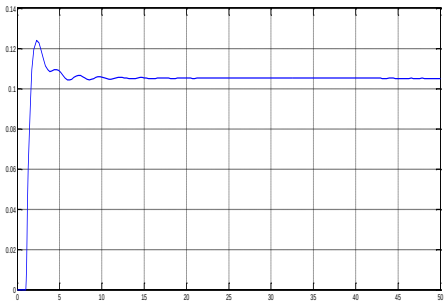	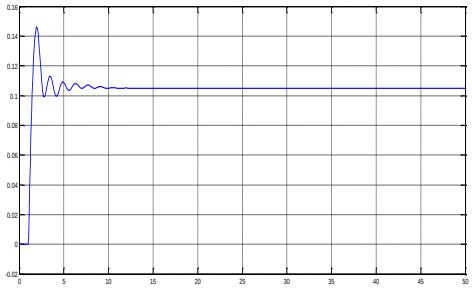
GENCO2	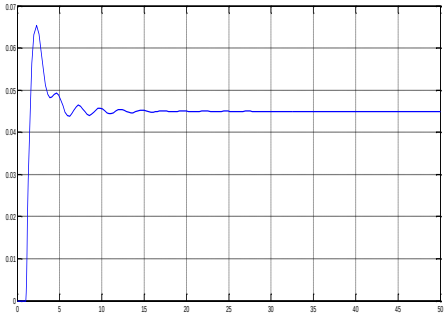	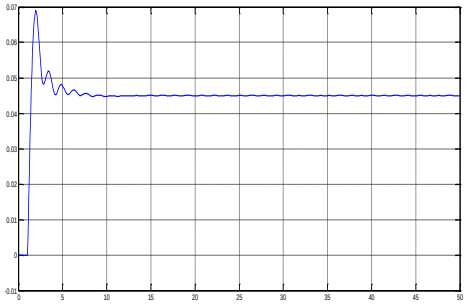
GENCO3	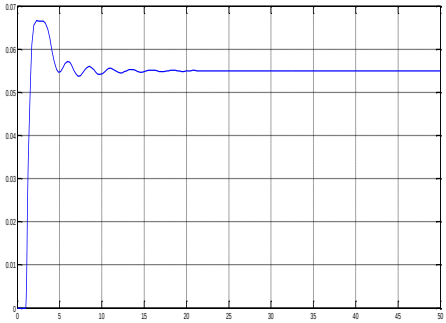	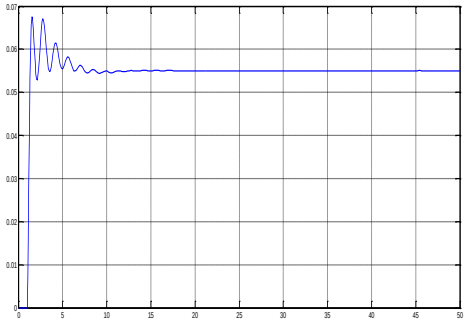
GENCO4	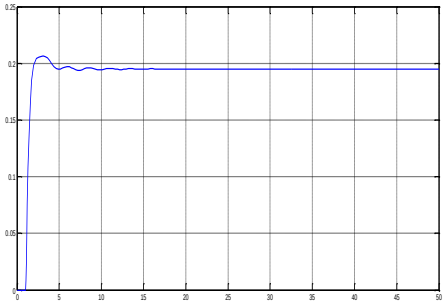	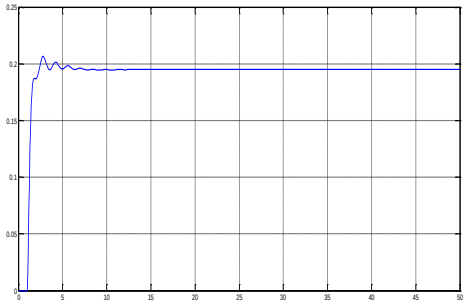

TABLE 7.22: Output response of genetic algorithm based two-area with non-linear governor in Deregulated Environment (with different apfs)

Parameters	**Non-linear Governor (Integral)**	**Non-linear Governor (PID)**
Δf_1	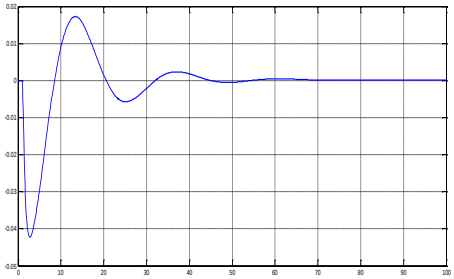	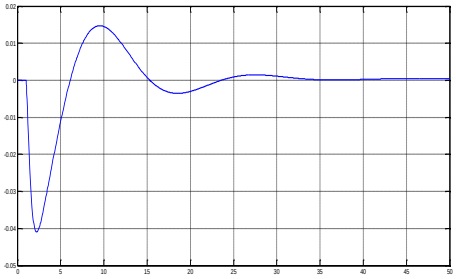
Δf_2	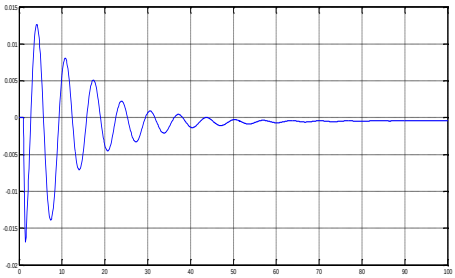	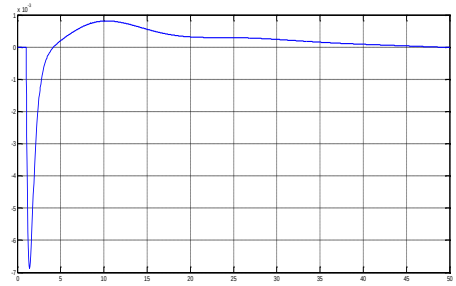
Tie-line	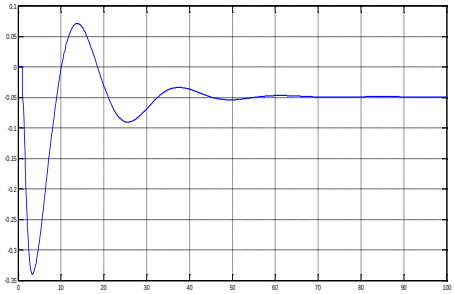	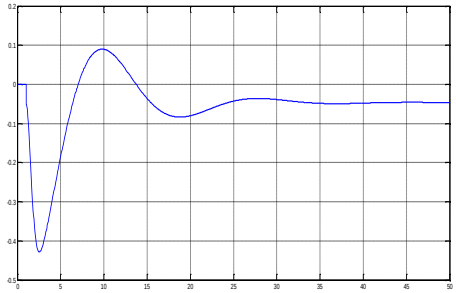
GENCO1	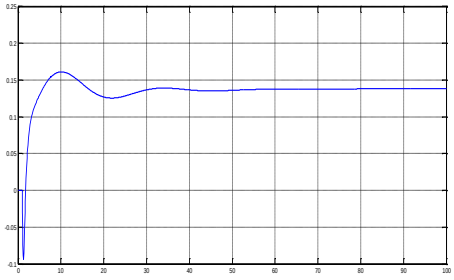	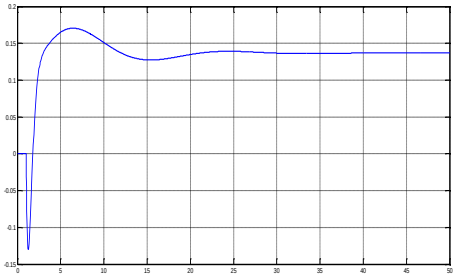

GENCO2	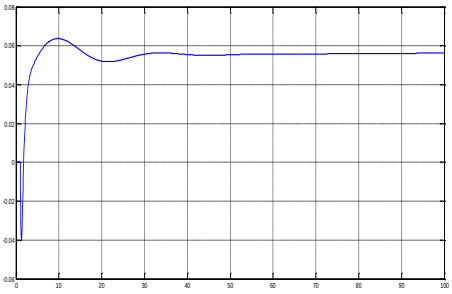	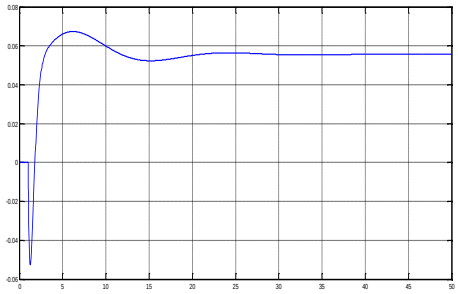
GENCO3	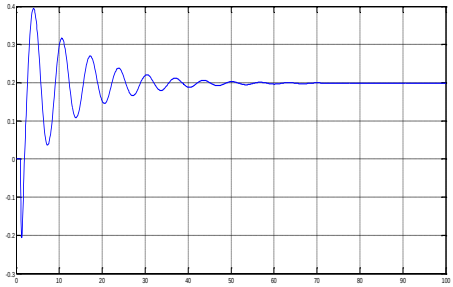	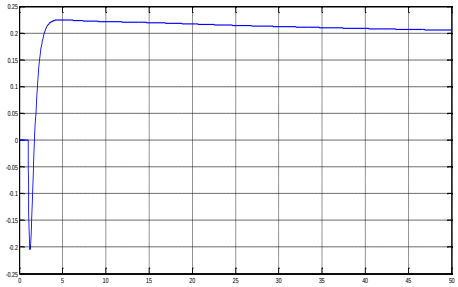
GENCO4	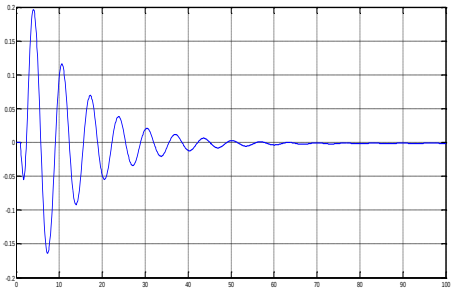	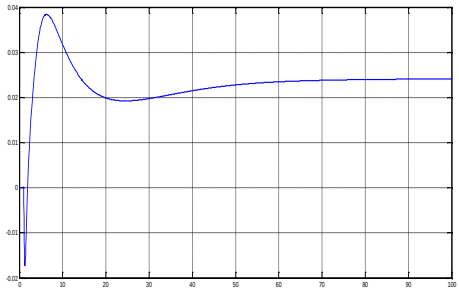

TABLE 7.23: Genetic Algorithm based gains of two-area with linear governor in Deregulated Environment (with different apfs)

Genetic Algorithm based optimal values				
Control Areas	Integral Controller	PID controller		
	K_i	K_p	K_i	K_D
Area-1	0.1787	0.4698	0.6687	0.7887
Area-2	0.2219	0.6445	0.7176	0.6789

TABLE 24: Genetic Algorithm based time response parameters of two-area with linear governor in Deregulated Environment (with different apfs)

Parameters	Overshoot	Undershoot	Settling time	Rise time	Delay time
With integral controller					
Δf_1	0.013	-0.055	25 sec	1.74 sec	1.2 sec
Δf_2	0.011	-0.035	30 sec	1.6 sec	1.15 sec
Tie-line	0	-0.075	25 sec	2.5 sec	2 sec
With PID controller					
Δf_1	0.011	-0.05	15 sec	1.6 sec	1.18 sec
Δf_2	0.008	-0.03	15 sec	1.4 sec	1.1 sec
Tie-line	0	-0.063	10 sec	3.6 sec	1.72 sec

TABLE 7.25: Genetic Algorithm based gains of two-area with non-linear governor in Deregulated Environment (with different apfs)

TCPS-SMES coordination with Integral Controller					
Area 1					
K_φ		T_{ps}		K_{i1}	
0.1748		0.1741		0.2790	
Area 2					
K_{SMES}	T_1	T_2	T_3	T_4	K_{i2}
0.6704	0.1	0.0164	0.1253	0.1702	0.0217

TCPS-SMES coordination with PID controller							
Area 1							
K_φ	T_{ps}		K_p	K_I	K_D		
0.1593	0.2576		0.0436	0.0352	0.0382		
Area 2							
K_{SMES}	T_1	T_2	T_3	T_4	K_p	K_I	K_D
0.0194	0.0248	0.0119	0.0986	0.0512	0.0269	0.0485	0.0180

TABLE 7.26: Genetic Algorithm based time response parameters of two-area with non-linear governor in Deregulated Environment (with different apfs)

Parameters	Overshoot	Undershoot	Settling time	Rise time	Delay time
With integral controller					
Δf_1	0.018	-0.042	70 sec	2.5 sec	1.16 sec
Δf_2	0.0126	-0.017	70 sec	1.6 sec	1.1 sec
Tie-line	0.072	-0.34	65 sec	4.5 sec	2.4 sec
With PID controller					
Δf_1	0.015	-0.041	30 sec	2.5 sec	1.8 sec
Δf_2	0.008	-0.006	20 sec	1.6 sec	1.1 sec
Tie-line	0.09	-0.425	30 sec	2.2 sec	1.28 sec

7.2.4.3 Scenario3: Contract Violation

According to the Case 3 discussed in the Section 5.7.3 the results of the load change: area frequency deviations, actual power flow on the tie-line and the generated powers of the various GENCOs following a step change in load demand of $DISCO_1$ and $DISCO_2$ for both linear and non-linear governor characteristics are shown below:

TABLE 7.27: Output response of genetic algorithm based two-area with linear governor in Deregulated Environment (contract violation)

Parameters	**Linear Governor (Integral)**	**Linear Governor (PID)**
Δf_1	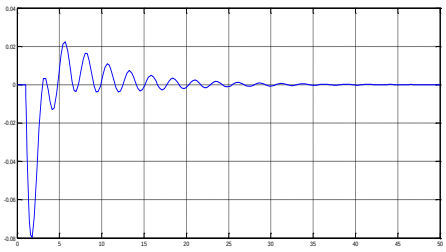	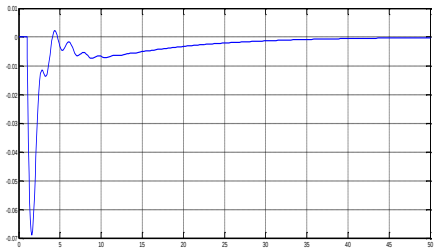
Δf_2	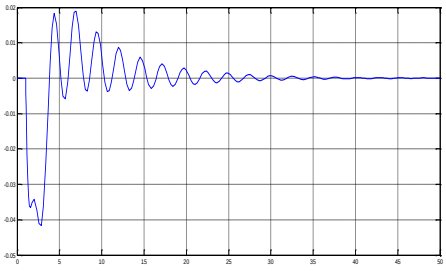	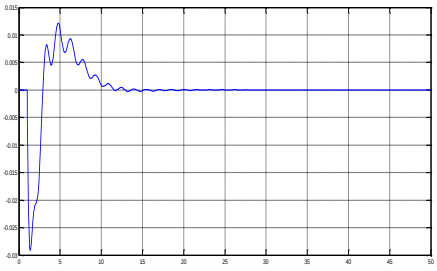

Tie-line	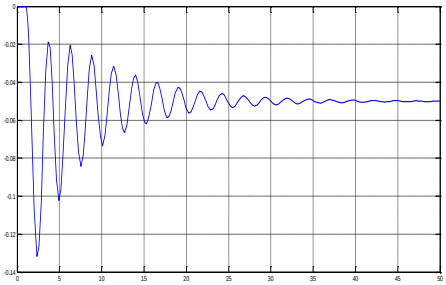	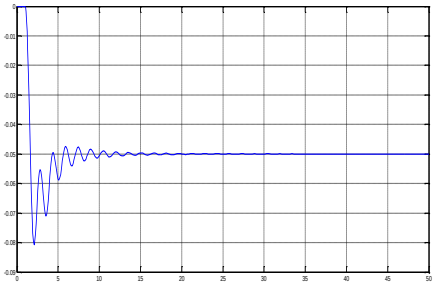
GENCO1	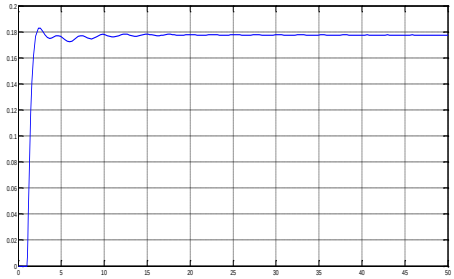	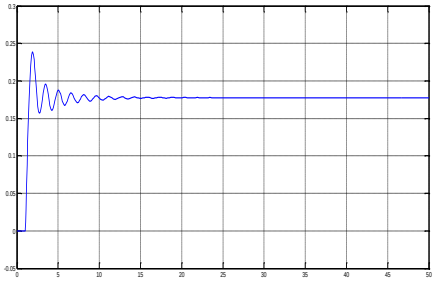
GENCO2	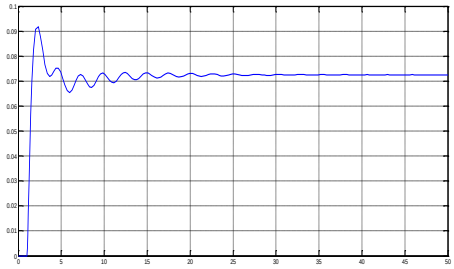	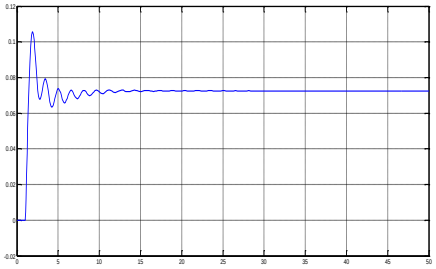
GENCO3	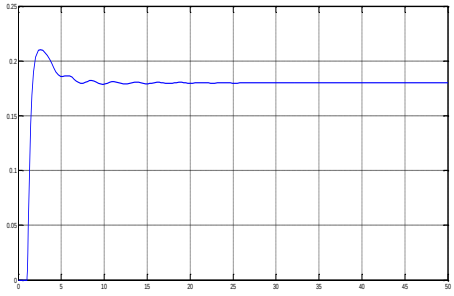	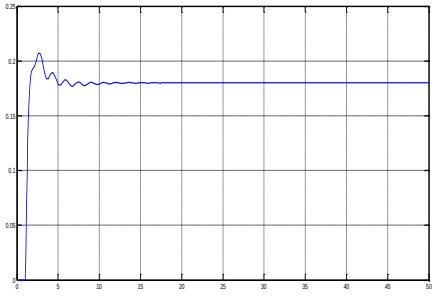
GENCO4	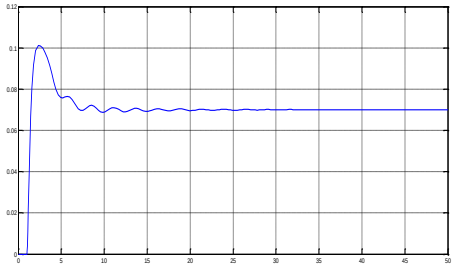	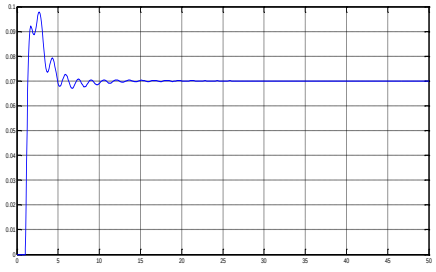

TABLE 7.28: Output response of genetic algorithm based two-area with non-linear governor in Deregulated Environment (contract violation)

Parameters	Non- linear Governor (integral)	Non-linear Governor (PID)
Δf_1	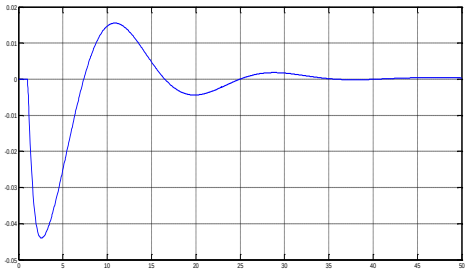	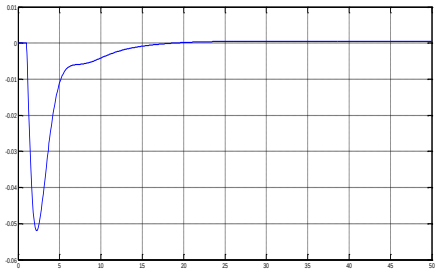
Δf_2	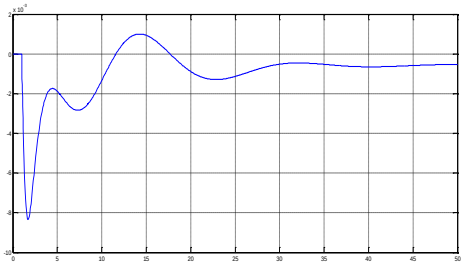	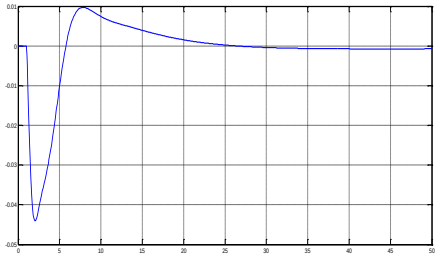
Tie-line	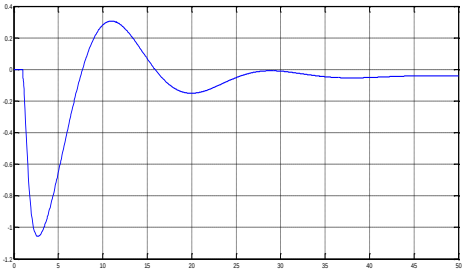	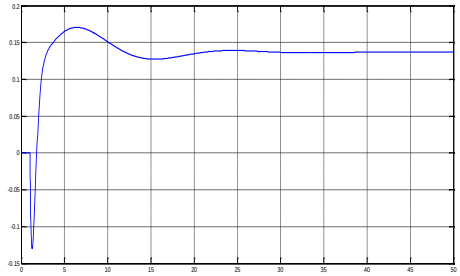
GENCO1	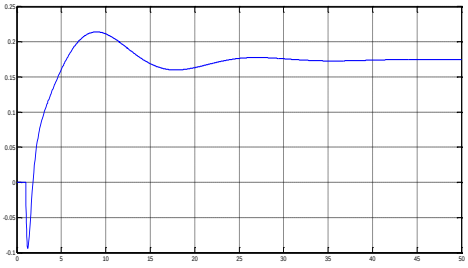	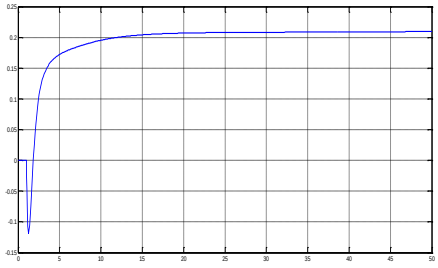

GENCO2	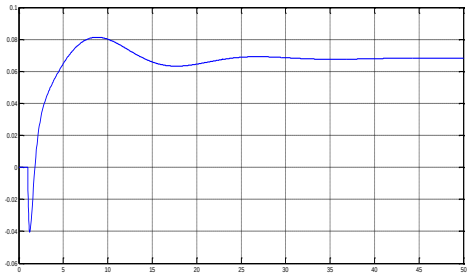	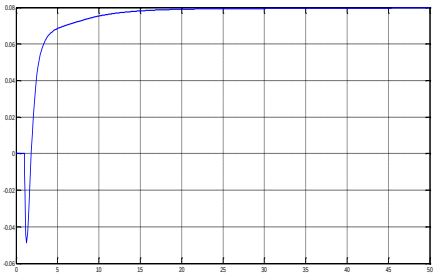
GENCO3	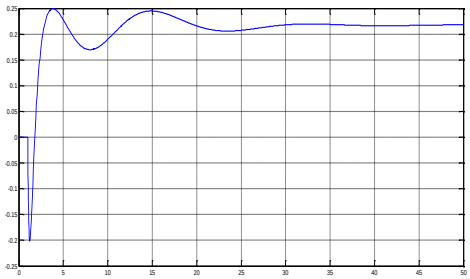	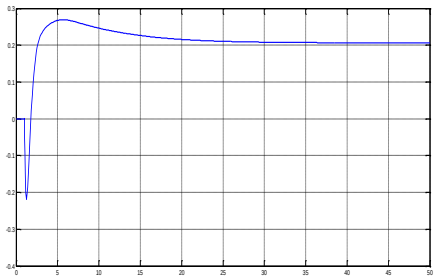
GENCO4	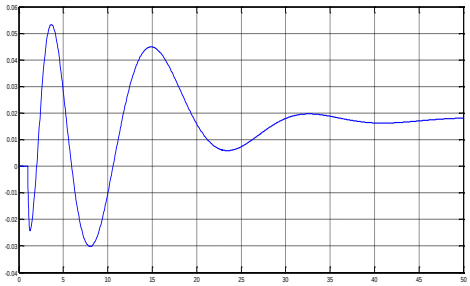	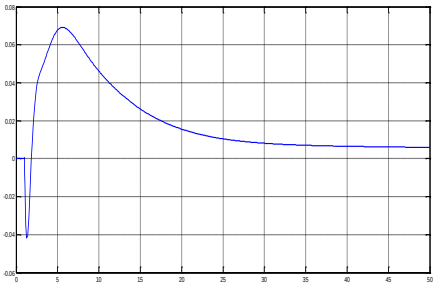

TABLE 7.29: Genetic Algorithm based gains of two-area with linear governor in Deregulated Environment (contract violation)

Genetic Algorithm based optimal values				
Control Areas	Integral Controller	PID controller		
	K_i	K_p	K_i	K_D
Area-1	0.2572	0.2335	0.1453	0.4523
Area-2	0.3831	0.4785	0.6864	0.3597

TABLE 7.30: Genetic Algorithm based time response parameters of two-area with linear governor in Deregulated Environment (contract violation)

Parameters	Overshoot	Undershoot	Settling time	Rise time	Delay time
With integral controller					
Δf_1	0.022	-0.08	40 sec	1.76 sec	1.2 sec
Δf_2	0.019	-0.04	45 sec	2.8 sec	1.15 sec
Tie-line	0	-0.132	50 sec	2.35 sec	1.67 sec
With PID controller					
Δf_1	0.005	-0.07	25 sec	1.5 sec	1.16 sec
Δf_2	0.012	-0.029	20 sec	2 sec	1.1 sec
Tie-line	0	-0.08	20 sec	2.15 sec	1.6 sec

TABLE 7.31: Genetic Algorithm based gains of two-area with non-linear governor in Deregulated Environment (contract violation)

TCPS-SMES coordination with Integral Controller					
Area 1					
K_φ		T_{ps}		K_{i1}	
0.3824		0.1108		0.1377	
Area 2					
K_{SMES}	T_1	T_2	T_3	T_4	K_{i2}
0.4630	0.1925	0.1582	0.1433	0.2410	0.2768

TCPS-SMES coordination with PID controller							
Area 1							
K_φ	T_{ps}			K_p	K_I	K_D	
0.1638	0.2746			0.0466	0.0416	0.0326	
Area 2							
K_{SMES}	T_1	T_2	T_3	T_4	K_p	K_I	K_D
0.2150	0.0954	0.1338	0.1637	0.1593	0.0485	0.0443	0.0441

TABLE 7.32: Genetic Algorithm based time response parameters of two-area with non-linear governor in Deregulated Environment (contract violation)

Parameters	Overshoot	Undershoot	Settling time	Rise time	Delay time
With integral controller					
Δf_1	0.016	-0.044	40 sec	2.9 sec	1.8 sec
Δf_2	0.001	-0.083	45 sec	1.7 sec	1.3 sec
Tie-line	0.31	-0.18	45 sec	2.5 sec	1.5 sec
With PID controller					
Δf_1	0.001	-0.052	20 sec	1.75 sec	1.1 sec
Δf_2	0.0097	-0.044	30 sec	1.8 sec	1 sec
Tie-line	0.001	-1.12	25 sec	2.1 sec	1.4 sec

The simulation results for two-area interconnected system for both linear and non-linear governor characteristics have been discussed. The response of the systems in Deregulated environment is also included. The Ziegler-nichols and Genetic Algorithm has been used for the stabilizing the output response of the system by taking adequate gain values.

CHAPTER 8

CONCLUSIONS & FUTURE SCOPE

8.1 CONCLUSION

The effectiveness of the AGC with linear and non-linear governor characteristics and the application of both in deregulated environment are investigated in the dissertation work. The step load perturbation to AGC with non-linear governor characteristics results in high frequency oscillations due to the positive real parts of some eigen value pairs and the system cannot attain the stable state. The coordinated TCPS-SMES is used for the stabilization of frequency and tie-line power oscillations. The optimized gains and parameters of the compensators obtained through genetic algorithm provide less overshoot and settling time with the help of PID controller as compared with Integral controller. It is emphasized that in restructured environment some adaptations are required in current AGC strategies for the satisfaction of different market structure and the specific distinctiveness of each power system.

8.2 FUTURE SCOPE

In the above research work, AGC with non-linear governor characteristics is developed by taking the consideration of market structure. The development helps in finding solutions to system problems. A proficient and more reliable power system is obtained with this work.

The new structure will be required for AGC system having improved compensators and intelligence technique for the controller gains to solve complex problems and other technical issues. This approach may be extended to multi area system including renewable energy sources.

REFERENCES

[1] Rabindra Kumar Sahu, Sidhartha Panda and Saroj Padhan," A hybrid firefly algorithm and pattern search technique for automatic generation control of multi area power systems," *International Journal of Electrical Power & Energy Systems*, Vol.64, pp.9-23, January 2015

[2] K.P. Singh Parmar, S.Majhi, D.P. Kothari," LFC of an interconnected power system with multi-source power generation in deregulated power environment," *International Journal of Electrical Power & Energy Systems,* Vol.57, pp. 277-286, May 2014.

[3] Swasti R. Khuntia, Sidhartha Panda," Simulation study for automatic generation control of a multi-area power systems by ANFIS approach," *Applied Soft Computing*, Vol.12, No.1, pp. 333-341, January 2012.

[4] Praghnesh Bhatt, Ranjit Roy and S.P. Ghoshal, "Automatic Generation Control of two-area interconnected hydro-hydro restructured power system with TCPS and SMES" *International Journal on Electrical and Power Engineering*, Vol.1, No.2, July 2010.

[5] Praghnesh Bhatt, Ranjit Roy and S.P. Ghoshal," Comparative performance evaluation of SMES-SMES, TCPS-SMES and SSSC-SMES controllers in automatic generation control for a two-area hydro-hydro system" *Electrical Power and Energy Systems* ,Vol.33, pp.1585-1597 February 2010.

[6] Katsuhiko Ogata, Modern Control Engineering, PHI, 5th Ed., 2010.

[7] B.S. Manke, Linear Control Systems, Khanna Publications, 2010.

[8] Anupama Huddar and P.S. Kulkarni,"A robust method of tuning the feedback gains of a variable structure load frequency controller using Genetic Algorithm optimization" *Electrical Power Components and Systems*, Vol.36, No.12, pp. 1351-1367, November 2008.

[9] Rajesh Joseph Abraham, D.Das and Amit Patra," Automatic generation control of an interconnected hydro thermal power system considering Superconducting magnetic energy storage," *Electrical Power & Energy Systems*, Vol.29, No.8, pp.571-579, October 2007

[10] Rajesh Joseph Abraham, D.Das, Amit Patra," AGC of a hydro-thermal system with Thyristor Controlled Phase Shifter in the tie-line", *IEEE Power India Conference*, 2006.

[11] Debapriya Das, Electrical Power Systems, New Age International, 2006.

[12] Ibraheem, Prabhat Kumar, D.P Kothari," Recent philosophies of automatic generation control strategies in power systems," *IEEE Transactions on Power System*, Vol.20, No.1, pp.346-357, February 2005.

[13] K.C. Divya and P.S. Nagendra Rao," A simulation model for AGC studies of hydro-hydro systems" *Electrical Power and Energy Systems*, Vol.27, pp. 335-342, December 2004.

[14] Hadi Sadaat, Power System Analysis, TATA McGraw Hill, New Delhi, 2002

[15] Vaibhav Donde, M.A Pai," Simulation and optimization in an AGC system after deregulation" *IEEE Transactions on Power Systems*, Vol.16, No.3, pp. 481-489, August 2001

[16] E.Nobile, Anjan Bose and Kevin Tomsovic," Bilateral Market for Load following ancillary services", in *Proc. PES Summer Power Meeting*, Seattle, W.A, pp. 704-706, July 2000

[17] S.C Tripathy, K.P Juengst," Sampled data automatic generation control with superconducting magnetic energy storage in power systems," *IEEE Transactions on Energy Conversion*, Vol.12, No.2, pp. 187-191, June 1997.

[18] Jayant Kumar, Kah-Hoe Ng and Gerald Sheble," AGC Simulator for Price Based Operation Part I: Model," *IEEE Transactions on Power Systems*, Vol.12, No.2, pp. 527-532, May 1997.

[19] Jayant Kumar, Kah-Hoe Ng and Gerald Sheble," AGC Simulator for Price Based Operation Part II: Case Study," *IEEE Transactions on Power Systems*, Vol.12, No.2, pp. 533-538, May 1997.

[20] Richard D. Christie and Anjan Bose," Load Frequency Control Issues in Power System Operations after Deregulation" *IEEE Transactions on Power Systems*, Vol.11, No.3, pp. 1191-1200, August 1996.

[21] I.J.Nagarath, D.P. Kothari, Power System Engineering, TATA McGraw Hill New York, 1994.

[22] P.Kundur, Power System Stability and Control, TATA McGraw Hill, New Delhi, 1994.

[23] N. Jaleeli, L.S. VanSlyck *et al*, "Understanding Automatic Generation Control", *IEEE Transactions on Power Systems*, Vol. 7, No. 3, pp. 1106-1122, August 1992.

[24] Kothari and Nanda, "Discrete- Mode Automatic Generation Control of Two-Area Reheat Thermal System" *IEEE Transactions on Power Systems*, Vol.4, No.2, pp. 70-71, May 1989.

[25] O.P Malik, Ashok Kumar, G.S Hope," A load frequency control algorithm based on generalized approach", *IEEE Transactions on Power Systems*, Vol.3, No.2, pp. 375-382, May 1988.

[26] T.M.Athay," Generation scheduling and control", *Proc.IEEE*, Vol.75, No.12, pp.1592-1606, December 1987

[27] H. G. Kwatny, K. C. Kalnitsky, and A. Bhatt, “An optimal tracking approach to load frequency control,” *IEEE Transactions on Power Systems*, Vol. PAS-94, No. 5, pp. 1635–1643, Sep./Oct.1975.

[28] IEEE Committee report,” Dynamic models for steam and hydro turbines in power in power system studies,” *IEEE Transactions on Power Apparatus and Systems*, Vol.92, No. 4, pp. 1904-1911, November 1973

[29] Cohn N. "Technique for improving the Bulk Power Transfers on Interconnected Systems ", *IEEE Transactions on Power Systems*, Vol.PAS-90, pp.2409-2419. November/December 1971

[30] C. Fosha and O. I. Elgerd, “The megawatt-frequency control problem: A new approach via optimal control theory,” *IEEE Transactions on Power Apparatus & Systems*, Vol. PAS-89, No. 4, pp. 563–577, April 1970.

APPENDIX- A

SYSTEM DATA

TABLE I (Thermal)		**TABLE II** (Hydro)	
$P_{r1}=P_{r2}$	2000MW	$H_1=H_2$	3 seconds
$H_1=H_2$	5 seconds	$D_1=D_2$	1
$D_1=D_2$	8.33*10^-3 p.uMW	$P_{r1}=P_{r2}$	1800 MW
$T_{T1}=T_{T2}$	0.3	$R_{p1}=R_{p2}$	0.05
$T_{G1}=T_{G2}$	0.08	$R_{T1}=R_{T2}$	0.05
R_1	2.4 Hz/p.uMW	$T_{G1}=T_{G2}$	0.2 seconds
P_{tiemax}	200MW	$T_{R1}=T_{R2}$	0.2 seconds
T_{12}*	0.545 p.uMW/Hz	T_{w1}	1 seconds

APPENDIX-B

Parameters	**Size**
Population size	20
No. of control variables	3
Crossover probability	0.9
Mutation Probability	0.1
Chromosome length	13